

## 2-Mercapto-quinazolinones as inhibitors of NDH-2 and *Mycobacterium tuberculosis*: Structure-activity relationships, mechanism of action and ADME characterization.

Dinakaran Murugesan, Peter C. Ray, Tracy Bayliss, Gareth A. Prosser, Justin R. Harrison, Kirsteen Green, Candice Soares de Melo, Tzu-Shean Feng, Leslie J. Street, Kelly Chibale, Digby F. Warner, Valerie Mizrahi, Ola Epemolu, Paul Scullion, Lucy Ellis, Jennifer Riley, Yoko Shishikura, Liam Ferguson, Maria Osuna-Cabello, Kevin D Read, Simon R. Green, Dirk A. Lamprecht, Peter M. Finin, Adrie J. C. Steyn, Thomas R. Ioerger, Jim Sacchettini, Kyu Y. Rhee, Kriti Arora, Clifton E. Barry, III, Paul G. Wyatt, and Helena Ingrid M. Boshoff

*ACS Infect. Dis.*, **Just Accepted Manuscript** • DOI: 10.1021/acsinfecdis.7b00275 • Publication Date (Web): 09 Mar 2018

Downloaded from <http://pubs.acs.org> on March 10, 2018

### Just Accepted

"Just Accepted" manuscripts have been peer-reviewed and accepted for publication. They are posted online prior to technical editing, formatting for publication and author proofing. The American Chemical Society provides "Just Accepted" as a service to the research community to expedite the dissemination of scientific material as soon as possible after acceptance. "Just Accepted" manuscripts appear in full in PDF format accompanied by an HTML abstract. "Just Accepted" manuscripts have been fully peer reviewed, but should not be considered the official version of record. They are citable by the Digital Object Identifier (DOI®). "Just Accepted" is an optional service offered to authors. Therefore, the "Just Accepted" Web site may not include all articles that will be published in the journal. After a manuscript is technically edited and formatted, it will be removed from the "Just Accepted" Web site and published as an ASAP article. Note that technical editing may introduce minor changes to the manuscript text and/or graphics which could affect content, and all legal disclaimers and ethical guidelines that apply to the journal pertain. ACS cannot be held responsible for errors or consequences arising from the use of information contained in these "Just Accepted" manuscripts.



1  
2  
3  
4  
5  
6  
7  
8  
9  
10  
11  
12  
13  
14  
15  
16  
17  
18  
19  
20  
21  
22  
23  
24  
25  
26  
27  
28  
29  
30  
31  
32  
33  
34  
35  
36  
37  
38  
39  
40  
41  
42  
43  
44  
45  
46  
47  
48  
49  
50  
51  
52  
53  
54  
55  
56  
57  
58  
59  
60

	Biological Chemistry and Drug Discovery College of Life Sciences Boshoff, Helena; NIAID, TBR

SCHOLARONE™  
Manuscripts

**2-Mercapto-quinazolinones as inhibitors of NDH-2 and *Mycobacterium tuberculosis*: Structure-activity relationships, mechanism of action and ADME characterization.**

Dinakaran Murugesan<sup>a,α</sup>, Peter C. Ray<sup>a,α</sup>, Tracy Bayliss<sup>a</sup>, Gareth A. Prosser<sup>b</sup>, Justin R. Harrison<sup>a</sup>, Kirsteen Green<sup>a</sup>, Candice Soares de Melo<sup>d</sup>, Tzu-Shean Feng<sup>d</sup>, Leslie J. Street<sup>d</sup>, Kelly Chibale<sup>d, c, e</sup>, Digby F. Warner<sup>f, c</sup>, Valerie Mizrahi<sup>f, c</sup>, Ola Epemolu<sup>a</sup>, Paul Scullion<sup>a</sup>, Lucy Ellis<sup>a</sup>, Jennifer Riley<sup>a</sup>, Yoko Shishikura<sup>a</sup>, Liam Ferguson<sup>a</sup>, Maria Osuna-Cabello<sup>a</sup>, Kevin D. Read<sup>a</sup>, Simon R. Green<sup>a</sup>, Dirk A. Lamprecht<sup>g</sup>, Peter M. Finin<sup>g,h</sup>, Adrie J.C. Steyn<sup>g,h</sup>, Thomas R. Ioerger<sup>i</sup>, Jim Sacchettini<sup>i</sup>, Kyu Y. Rhee<sup>j</sup>, Kriti Arora<sup>b</sup>, Clifton E. Barry III<sup>b,c</sup>, Paul G. Wyatt<sup>\*a</sup> and Helena I.M. Boshoff<sup>\*b</sup>

<sup>a</sup>Drug Discovery Unit, Division of Biological Chemistry and Drug Discovery, School of Life Sciences, University of Dundee, Sir James Black Centre, Dundee, DD1 5EH, UK

<sup>b</sup>Tuberculosis Research Section, Laboratory of Clinical Immunology and Microbiology, National Institute of Allergy and Infectious Disease, National Institutes of Health, 9000 Rockville Pike, Bethesda, MD, 20892, USA

<sup>c</sup>Institute of Infectious Disease and Molecular Medicine, University of Cape Town, Rondebosch, South Africa

<sup>d</sup>Drug Discovery and Development Centre (H3D), Department of Chemistry, University of Cape Town, Rondebosch 7701, South Africa

<sup>e</sup>South African Medical Research Council Drug Discovery and Development Research Unit, Department of Chemistry, University of Cape Town, Rondebosch 7701, South Africa

<sup>f</sup>SAMRC/NHLS/UCT Molecular Mycobacteriology Research Unit & DST/NRF Centre of Excellence for Biomedical TB Research, Dept. of Pathology, Faculty of Health Sciences, University of Cape Town, Rondebosch 7701, South Africa

<sup>g</sup>Africa Health Research Institute (AHRI), K-RITH Tower Building Level 3, 719 Umbilo Road, Durban 4001, South Africa

<sup>h</sup>Department of Microbiology, University of Alabama at Birmingham, 1720 2nd Avenue South, Birmingham, Alabama 35294-2170, USA

<sup>i</sup>Department of Computer Science and Engineering, Texas A&M University, College Station, TX, USA

<sup>j</sup>Division of Infectious Diseases, Weill Department of Medicine, Weill Cornell Medical College, NY, NY 10065, USA

<sup>‡</sup>Current address: Department of Internal Medicine, University of Pittsburgh, 1218 Scaife Hall 3550 Terrace Street, Pittsburgh, Pennsylvania 15261, USA

\*Corresponding authors, <sup>α</sup>contributed equally  
[hboshoff@niaid.nih.gov](mailto:hboshoff@niaid.nih.gov); P.G.Wyatt@dundee.ac.uk

*Mycobacterium tuberculosis* (*MTb*) possesses two non-proton pumping type II NADH dehydrogenase (NDH-2) enzymes which are predicted to be jointly essential for respiratory metabolism. Furthermore, the structure of a closely related bacterial NDH-2 has been reported recently, allowing for the structure-based design of small-molecule inhibitors. Herein, we disclose *MTb* whole-cell structure-activity relationships (SAR) for a series of 2-mercapto-quinazolinones which target the *ndh* encoded NDH-2 with nanomolar potencies. The compounds were inactivated by glutathione-dependent adduct formation as well as quinazolinone oxidation in microsomes. Pharmacokinetic studies demonstrated modest bioavailability and compound exposures. Resistance to the compounds in *MTb* was conferred by promoter mutations in the alternative non-essential NDH-2 encoded by *ndhA* in *MTb*. Bioenergetic analyses revealed a decrease in oxygen consumption rates in response to inhibitor in cells in which membrane potential was uncoupled from ATP production, while inverted membrane vesicles showed mercapto-quinazolinone-dependent inhibition of ATP production when NADH was the electron donor to the respiratory chain. Enzyme kinetic studies further demonstrated non-competitive inhibition, suggesting binding of this scaffold to an allosteric site. In summary, while the initial *MTb* SAR showed limited improvement in potency, these results, combined with structural information of the bacterial protein, will aid in the future discovery of new and improved NDH-2 inhibitors.

**KEYWORDS**

1  
2  
3 *Mycobacterium tuberculosis*, mercapto-quinazolinones, structure-activity relationship (SAR), type II NADH  
4 dehydrogenase (NDH-2), small molecule NDH-2 inhibitors, respiration  
5  
6  
7  
8  
9

10       Tuberculosis (TB) is a major global health problem, resulting in significant morbidity each year.  
11  
12 Although mortality has fallen dramatically since 1990, TB now ranks alongside HIV as a leading cause of  
13 death worldwide. While HIV-related deaths have been declining largely as a result of improved access to,  
14 and availability of, better HIV treatments, this has not been the case for TB <sup>1</sup>, the treatment of which  
15 requires 6 months of chemotherapy with a combination of four agents (isoniazid, rifampicin, pyrazinamide  
16 and ethambutol) to achieve durable cure of drug-sensitive TB <sup>2</sup>. The large number of TB patients, coupled  
17 with the chemotherapeutic burden, often leads to poor patient adherence and sub-optimal treatment  
18 outcomes in the developing world, as well as the emergence of multi-drug resistant TB (MDR-TB, defined as  
19 resistance to isoniazid (INH) and rifampicin (RIF)) and extensively drug-resistant tuberculosis (XDR-TB,  
20 defined as MDR-TB plus resistance to any fluoroquinolone and one of three second-line injectable drugs,  
21 capreomycin, kanamycin (Kan), and amikacin). To address this global TB health problem, an improved  
22 treatment regimen is needed which will reduce treatment duration, and prevent relapse and the  
23 development of TB drug resistance <sup>3-8</sup>. However, achieving this goal will require discovery of multiple novel  
24 and mechanistically distinct anti-mycobacterial agents possessing reduced liabilities for investigation of  
25 new drug regimens that might shorten the duration of treatment, and simplify management of the disease  
26 by improving adherence and reducing costs <sup>9-12</sup>.  
27  
28  
29  
30  
31  
32  
33  
34  
35  
36  
37  
38  
39  
40  
41  
42  
43  
44

45       Identification of novel drug targets that will lead to treatment shortening is challenging. Targets of  
46 drugs currently in use or phase 3 clinical evaluation for TB chemotherapy include cell wall biosynthesis,  
47 translation, transcription, folate synthesis, ATP generation and maintenance of DNA topology as broad  
48 categories, although the nitroimidazoles delamanid and pretomanid, generate reactive nitrogen  
49 intermediates that inhibit several essential processes <sup>13</sup>. Mechanistically novel drugs would conceptually  
50 target distinct processes from the above and to date, successes in the field have all emerged from target  
51 identification of hits discovered in *Mtb* whole cell screens <sup>13</sup>.  
52  
53  
54  
55  
56  
57  
58  
59  
60

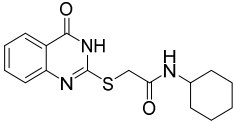
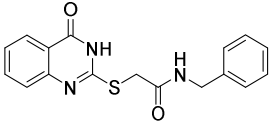
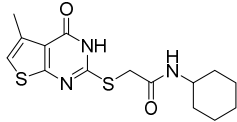
In this work, we describe the identification of a 2-mercapto-quinazoline scaffold identified from a *MTb* whole cell screen, which had been previously reported to inhibit the mycobacterial type II NADH dehydrogenase<sup>14</sup>; providing further evidence for its inhibition of the *MTb* NDH-2. *MTb* encodes two NDH-2 genes of which the one encoded by *ndh* is play a critical role for growth both *in vitro* and *in vivo*<sup>15-17</sup>. NDH-2 catalyses the transfer of electrons from NADH into the mycobacterial respiratory pathway and has been proposed to be targeted by a number of early stage inhibitors<sup>16, 18-20</sup>. In contrast, the proton pumping type I NADH dehydrogenase can be deleted without apparent effects on growth both *in vitro* or *in vivo*<sup>15-17</sup>. As the current series was considered to have a promising drug-like profile (Table 1), a focused optimization program was initiated.

RESULTS AND DISCUSSION

Screening of a commercial diversity library, details of which will be published elsewhere, afforded a 2-mercapto-quinazolinone cluster of hits (**1**, **2** and **3**), with compounds **1** and **2** showing potent *MTb* whole-cell minimum inhibitory concentration (MIC) in two distinct growth media. The compounds were assessed in a series of early stage biology profiling assays to understand better the mechanism of action (MoA). These included screening the compounds against a *cyd* knockout strain which is known to be hyper-susceptible to inhibitors of the cytochrome *bc*<sub>1</sub> complex<sup>21</sup>, which suggested that the series was unlikely to target QcrB. Profiling also investigated the extent of upregulation of the promoter of the *iniBAC* gene cluster, known to be induced by inhibitors of cell wall biosynthesis, such as isoniazid, ethionamide, SQ109 and ethambutol<sup>22-23</sup>, which suggested **1** and **2** did not have an effect on cell wall biosynthesis. These biology profiling data were considered promising, especially in conjunction with a recent report<sup>14</sup> in which mutations in *MTb* mutants spontaneously resistant to compound **1** mapped to *ndhA*, the gene encoding the non-essential type-II NADH dehydrogenase that is involved in NADH re-oxidation in the mycobacterial oxidative phosphorylation pathway<sup>14</sup>. There are two closely related non-proton pumping type II NADH dehydrogenases in the *MTb* genome, of which only one (encoded by *ndh*, Rv1854c) is essential<sup>24-27</sup>. Iorger

*et al.*<sup>14</sup> identified promoter mutations in *ndhA* which resulted in >40 fold upregulation of gene expression, likely compensating for compound **1** inhibiting the essential NDH-2 homolog.

**Table 1:** Profiling of confirmed hits **1**, **2** and **3**

Confirmed hits			
	<b>1</b>	<b>2</b>	<b>3</b>
GAST MIC (μM)	0.3	5.9	43
7H9-ADC MIC (μM)	0.6	4.5	>50
GAST LLE	4.2	3.5	1.7
Cyd KO reporter	Not likely QcrB inhibitor	Not likely QcrB inhibitor	-
<i>pini</i> -LUC reporter	Not likely cell wall inhibitor	Not likely cell wall inhibitor	-
HepG2 IC <sub>50</sub> (μM)	> 50	-	-
CHI-LogD	1.8	1.5	-
Microsomal Cli (mL/min/g)	Mouse 2.3 Human <0.5	Mouse 1.6	-
MW <sup>a</sup>	317	325	337
clogP <sup>a</sup> / clogD <sup>a</sup>	2.3 / 2.3	1.7 / 1.7	2.7 / 2.7
TPSA <sup>a</sup>	75	75	75
Kin. solubility (μM) <sup>b</sup>	83	109	-
PFI	4.7	4.3	4.7

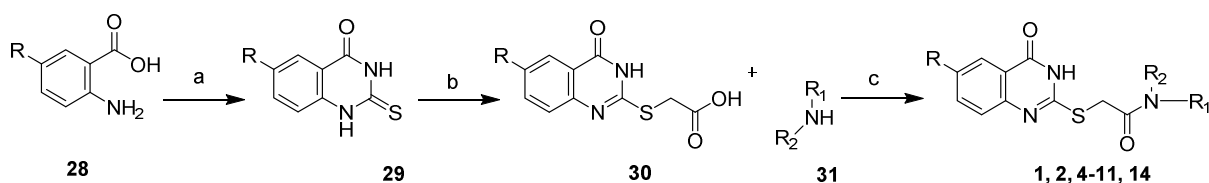
<sup>a</sup> Calculated using StarDrop (<http://www.optibrium.com>).

<sup>b</sup> Kinetic aqueous solubility was measured using laser nephelometry of compounds in 2.5% DMSO.

Compound **1** had a promising *MTb* MIC-derived ligand-lipophilicity efficiency (LLE) drug-likeness profile, suggestive of a quality starting point for medicinal chemistry optimisation<sup>28-29</sup>. Compound **1** also showed no noticeable cytotoxicity in a mammalian cell line (HepG2). Compounds **1** and **2** also had moderate kinetic solubility and reasonable mouse hepatic microsomal stability, with **1** having excellent human microsomal stability (Table 1). Herein, we report on the development of the structure-activity relationship (SAR) for **1**, as well as extended ADME characterisation of key compounds.

**Synthetic chemistry:** Quinazolinone amides reported herein were synthesized utilizing known procedures, which are detailed in Scheme 1. Commercially available anthranilic acids (**28**) were cyclized with thiourea, and the resulting 2-mercapto quinazoline-4-diones (**29**) or commercially available 2-mercapto-4(3H)-quinazolinone was reacted with 2-bromo acetic acid to form the 2-((4-oxo-3,4-dihydroquinazolin-2-yl)thio)acetic acids (**30**). Primary and secondary amines (**31**) were coupled using standard coupling reagents to afford compounds **1**, **2**, **4-11** and **14**.

**Scheme 1.** General synthetic route for synthesis of quinazolinone amides



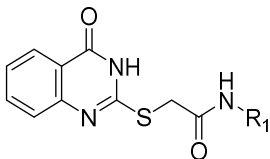
**Reagents and conditions:** General synthetic approach to quinazolinones **1**, **2**, **4-11** and **14**. (a) neat thiourea at 180°C, 3 h; (b) 2-bromoacetic acid, triethylamine, DMF, 80°C, 12 h; (c) primary and/or secondary amine **31**, EDC·HCl, HOAT, *N,N*-diisopropylethylamine, DMF:ACN 1:1, room temperature, 12 h; or primary and/or secondary amine **31**, HATU, *N,N*-diisopropylethylamine, DCM, room temperature, 12 h.

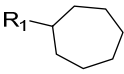
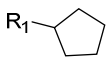
**MTb whole-cell SAR:** The initial medicinal chemistry plan focussed on developing the SAR with the aim of better understanding the pharmacophore. Initial efforts were guided by mouse microsomal metabolite identification (met-ID) studies on **1**, which revealed significant oxidation of the cyclohexyl and quinazolin-4(3H)-one rings as well as cleavage of the amide bond (Figure S1). To understand the scope, cycloalkyls **4**, **5** and **6** were prepared (Table 2). The large bulky lipophilic cyclohexyl **1** and cycloheptyl **4** were both equally favoured, with good whole-cell MIC potency. In contrast, the smaller ring-contracted cyclopentyl **5** and cyclobutyl **6** were slightly less potent (Table 2), and the cyclopropyl and ring deletion NHMe analogues (data not shown) resulted in a complete loss of whole-cell activity, suggesting that a bulky hydrophobic group was required to obtain good whole-cell potency. As mouse met-ID of **1** showed significant oxidation of the cyclohexyl group, the 2-, 3- and 4-hydroxylated cyclohexyl derivatives were prepared with the aim of improving solubility as well as microsomal stability. Improvements in both kinetic

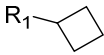
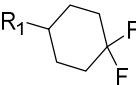
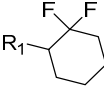
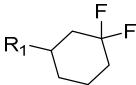
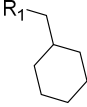
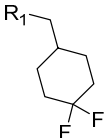


solubility and mouse microsomal stability were indeed achieved, but no whole-cell activity was observed (data not shown). An additional focussed set of polar saturated 4-, 5-, and 6-membered oxygen-containing saturated heterocycles was prepared; however, whilst having good kinetic solubility and mouse microsomal stability, they too lost all whole-cell activity (data not shown). There were also attempts to improve solubility with differentially functionalised 4-substituted piperidines (NAc, NSO<sub>2</sub>Me, NMe and NBn) but, once again, there was a loss of whole-cell activity (data not shown). As the cyclohexyl group within **1** did not appear to tolerate polar solubilising groups, we turned our focus to introducing fluorine in an attempt to improve microsomal stability<sup>30-31</sup>. We were encouraged to find that the 4, 4-difluorocyclohexan **7** retained good whole-cell potency, and also had slightly improved mouse microsomal stability versus **1**. In comparison to **1**, mouse microsomal met-ID on **7** showed a small amount of amide bond cleavage as well as oxidation of the quinazolin-4(3H)-one ring (Figure S2). The 2, 2- and 3, 3-difluorocyclohexan compounds **8** and **9** had moderate to poor whole-cell potency. Met-ID for both **1** and **7** revealed cleavage of the amide bond, so attempts to hinder the amide through formation of the 1- methyl-, 1-methanol- and 1-cyano-substituted cyclohexane were explored, all of which resulted in a complete loss of MIC potency as well as increased mouse microsomal instability (data not shown). Addition of a methylene bridge in **1** and **7** to afford **10** and **11** improved MIC potency, further emphasising the requirement for bulky lipophilic groups.

**Table 2:** Evaluation R1 (cyclohexyl) SAR.



ID	R <sub>1</sub>	H37Rv MIC <sup>a</sup>		cLogP	Mouse Cl <sup>b</sup> (mL/min/g)	Solubility <sup>c</sup> (μM)
		GAST	(μM) 7H9-ADC			
<b>4</b>		0.3	0.6	2.9	6.4	39
<b>5</b>		1.0	1.8	1.6	2.5	101

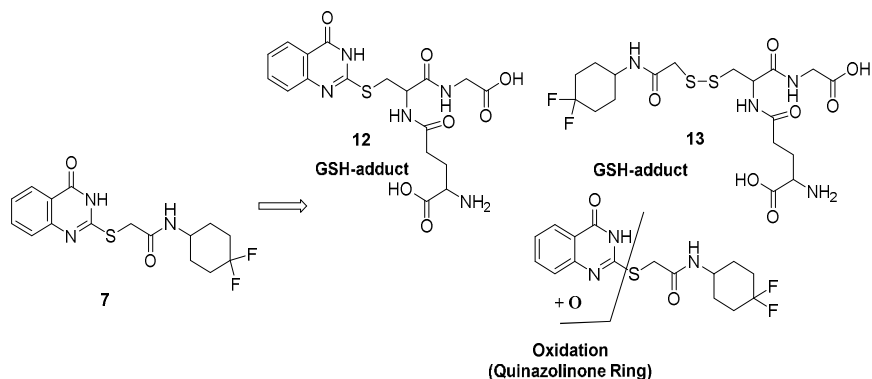
6		1.6	1.6	1.2	1.8	219
7		0.4	0.4	2.3	1.4	105
8		9.4	12.5	2.3	2.3	219
9		4.7	4.7	2.3	2.9	187
10		0.2	0.3	2.6	5.9	-
11		0.8	1.1	2.6	4.7	250

<sup>a</sup>Minimum inhibitory concentration (MIC) is the minimum concentration required to inhibit >99% growth of *M. tuberculosis* in liquid culture.

Isoniazid was included as an internal control reference compound (MIC of 0.2 ± 0.1 μM). <sup>b</sup>Intrinsic clearance (Cl<sub>i</sub>) using CD1 mouse liver microsomes.

<sup>c</sup>Kinetic aqueous solubility was measured using laser nephelometry of compounds in 2.5% DMSO.

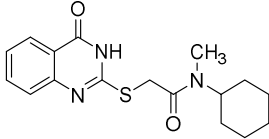
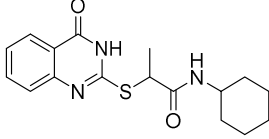
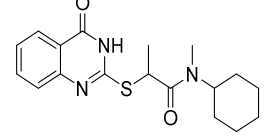
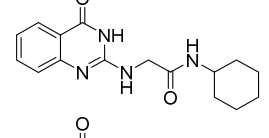
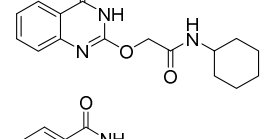
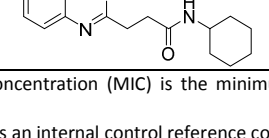
There were concerns over the *S*-linker, based on previous experience from whole-cell screening where confirmed hits with similar *S*-linker compounds were found to react with glutathione (GSH) both with and without microsomal activation. GSH trapping on **7**, with and without human liver microsomes (Figure S3) showed GSH adducts **12** and **13**, without microsomal activation. It is presumed that GSH results in cleavage of the sulphur-quinazolinone **7** linker, to afford **12**, with GSH coupling to the displaced *S*-Linker to afford **13**. Human microsomal oxidation of the quinazolinone ring of **7** was also observed (see Figure 1).



**Figure 1. Metabolite identification of 7 in a GSH trapping experiment.**

Whilst the level of GSH adduct formation for **7** was relatively low and no HepG2 cytotoxicity was observed, this was considered a liability of the series as the reactivity did not require microsomal activation and the ability to predict and quantify the risk of idiosyncratic adverse drug reactions is limited<sup>32-33</sup>. We attempted to reduce this liability by modifying the linker. *N*-methylation of the amide and/or the methylene linker to afford **14**, **15** and **16**, was not tolerated. The NH-, *O*- and CH<sub>2</sub>-linkers were readily prepared to afford **17**, **18** and **19**. However all resulted in a loss of MIC potency (see Table 3). Oxidation of S-atom in compound **1** was attempted using a variety of conditions and oxidation reagents (for example 3-chlorobenzoic acid, potassium permanganate and Oxone). However, all attempts failed to deliver the desired sulfone, possibly as a result of increased reactivity.

**Table 3:** Evaluation of S-linker SAR.

ID	Structure	H37Rv MIC <sup>a</sup>		cLogP	Mouse CLi <sup>b</sup> mL/min/g	Solubility <sup>c</sup> μM
		GAST	7H9-ADC			
<b>14</b>		50	50	2.4	13	250
<b>15</b>		50	50	2.6	7.5	250
<b>16</b>		50	50	2.9	50	250
<b>17</b>		50	50	1.9	2.1	250
<b>18</b>		25	50	1.2	-	-
<b>19</b>		50	50	2.1	1.6	250

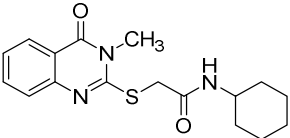
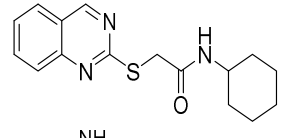
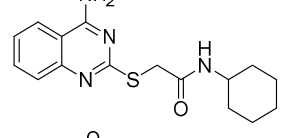
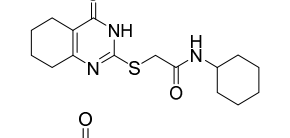
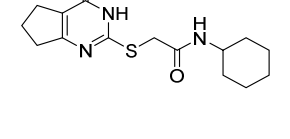
<sup>a</sup>Minimum inhibitory concentration (MIC) is the minimum concentration required to inhibit >99% growth of *M. tuberculosis* in liquid culture.

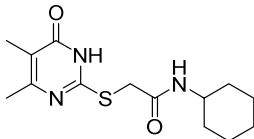
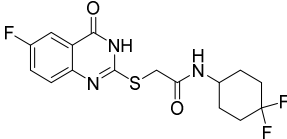
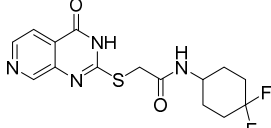
Isoniazid was included as an internal control reference compound (MIC of 0.2 ± 0.1 μM). <sup>b</sup>Intrinsic clearance (CLi) using CD1 mouse liver microsomes.

<sup>c</sup>Kinetic aqueous solubility was measured using laser nephelometry of compounds in 2.5% DMSO.

Changes to the quinazolinone ring were then explored, starting with *N*-methylation to afford **20**, which was not tolerated. Removal of the carbonyl, by synthesis of quinazoline **21** and quinazolin-4-amine **22**, was also not tolerated. Saturation of the quinazolinone core phenyl afforded **23**, which retained good MIC potency and also resulted in improved solubility; albeit microsomal stability was poor. The related 5-membered saturated analogue **24** showed similar MIC potency, but with improved microsomal stability as well as solubility. However, the di-methyl analogue **25** was less well tolerated, suggesting that a bulky hydrophobic ring was preferred. The above SAR suggested that the pyrimidinone core was a key part of the pharmacophore. As human-metID showed oxidation of the quinazolinone ring of **7**, we synthesized the presumably more stable fluorine analogue **26** which, whilst not as potent as **7**, retained good MIC potency. However, the solubility was poor and the mouse microsomal stability moderate. In an attempt to improve solubility as well as microsomal stability, the pyridopyrimidinone **27** was prepared; whilst solubility and microsomal stability were improved, the compound had moderate to weak MIC potency.

**Table 4:** Evaluation of quinazolinone core.

ID	Structure	H37Rv MIC <sup>a</sup> (μM)		cLogP	Mouse CL <sub>50</sub> <sup>b</sup> (mL/min/g)	Solubility <sup>c</sup> (μM)
		GAST	7H9-ADC			
20		50	50	2.9	11	-
21		50	50	3.8	-	-
22		50	50	3.8	-	-
23		1.2	1.6	2.2	6.6	250
24		1.6	1.2	1.8	1.2	250

25		6.3	12.5	2.1	1.1	250
26		0.6	0.8	2.4	2.2	55
27		9.4	2.5	1.2	1.6	250

<sup>a</sup>Minimum inhibitory concentration (MIC) is the minimum concentration required to inhibit >99% growth of *M. tuberculosis* in liquid culture.

Isoniazid was included as an internal control reference compound (MIC of  $0.2 \pm 0.1 \mu\text{M}$ ). <sup>b</sup>Intrinsic clearance (C<sub>li</sub>) using CD1 mouse liver microsomes.

<sup>c</sup>Kinetic aqueous solubility was measured using laser nephelometry of compounds in 2.5% DMSO.

A summary of the overall whole-cell SAR for **1**, as well as the effects on both kinetic solubility and microsomal stability, is shown in Figure 2 and in Tables 2-4.

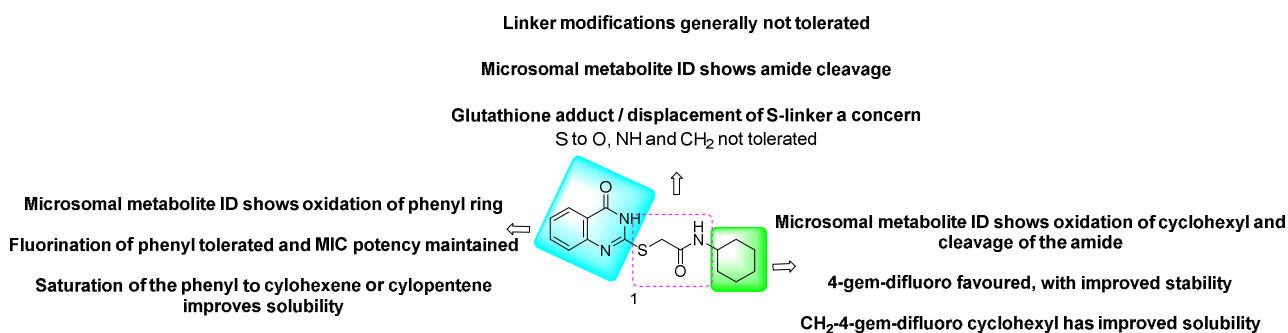


**Figure 2.** Overview of structure-activity and property relationships of the mercapto-quinazolinones.

Pharmacokinetic studies were initiated in order to assess the potential for *in vivo* efficacy studies of the 2-mercapto-quinazolinones. Compound **1**, when dosed as the free base, had reasonable bioavailability, consistent with its moderate C<sub>li</sub> and solubility, and good permeability (Table 5). Compound **7** showed a similar bioavailability and exposure profile to **1** (Table 5).

**Table 5:** Pharmacokinetic profiling of compounds **1**, **7** and **11**.

	<b>1</b>	<b>7</b>	<b>11</b>
--	----------	----------	-----------

<b>GAST MIC (μM)</b>	0.3 (95 ng/mL)	0.4 (141 ng/mL)	0.8 (294 ng/mL)
<b>7H9-ADC MIC (μM)</b>	0.6 (190 ng/mL)	0.4 (141 ng/mL)	0.8 (294 ng/mL)
<b>HepG2 IC<sub>50</sub> (μM)</b>	> 50	>50	>50
<b>Measured CHI-LogD</b>	1.8	1.5	1.6
<b>Microsomal clearance (ml/min/g)</b>	Mouse 2.3 Human <0.5	Mouse 1.4	Mouse 4.8
<b>MW<sup>a</sup></b>	317	353	367
<b>clogP<sup>a</sup> / clogD<sup>a</sup></b>	2.3/2.3	2.3/2.3	2.7/2.7
<b>TPSA<sup>a</sup></b>	75	75	75
<b>PAMPA</b>	83 (nm/sec)	64 (nm/sec)	65 (nm/sec)
<b>Kinetic solubility (μM)<sup>b</sup></b>	83 (free base)	111 (HCl salt)	>250
<b>C57 Mouse PK at 3 iv &amp; 10 po (mg/kg)</b>	Free base	HCl salt	Free base
<b>C<sub>max</sub> (ng/ml)</b>	748	399	1112
<b>T<sub>1/2</sub> h</b>	1.5	1.3	
<b>AUC<sub>0-8h</sub> (ng.min/ml)</b>	156800	67085	128309
<b>Cl<sub>b</sub> (ml/min/kg)</b>	23	39	
<b>Vd<sub>ss</sub> (L/kg)</b>	0.8	1	
<b>%F</b>	46	29	
<b>PPB (% unbound)</b>	14	13	21

<sup>a</sup> Calculated using StarDrop (<http://www.optibrium.com>).

<sup>b</sup>Kinetic aqueous solubility was measured using laser nephelometry of compounds in 2.5% DMSO.

As compound **7** had comparable MIC potency, mouse microsomal stability and pharmacokinetic profile to **1**; a dose linearity study was conducted to evaluate if exposures above the MIC could be achieved. However, no dose linearity was observed between the 30 and 100 mg/kg doses, determined by the area under the curve (AUC) comparison (Figure S4). This may be a consequence of solubility limited absorption at the highest dose. Compound **11** demonstrated better kinetic solubility and comparable MIC to compounds **1** and **7**, yet despite an improved C<sub>max</sub> and T<sub>max</sub> compared to compound **1**, likely driven by its improved kinetic solubility, it had a lower exposure (AUC) over time (Figure S5 and Table 5), likely a consequence of it's higher clearance (Mouse Cl<sub>i</sub> 4.7 mL/min/g versus 2.3 or 1.4 for compound **1** and **7**, respectively). The modest compound exposures upon oral dosing, combined with the lack of *ex vivo* intra-macrophage efficacy (*vide infra*), suggested that efficacy studies of these compounds in infected mice were unlikely to validate the target/drug candidate pair in an animal model where the disease is macrophage-based. As such an efficacy experiment was not performed.

*Biological characterization of the mercapto-quinazolinones*

Previous work on a mercapto-quinazolinone had suggested that compound **1** might target NDH-2 as evidenced by promoter mutations in the non-essential *ndhA* gene encoding an orthologue of the type II NADH dehydrogenase<sup>14</sup>. We similarly identified promoter mutations for *ndhA* but were not able to identify polymorphisms in the apparently essential *ndh* (Rv1854c) (Table S1) suggesting that mutations were either deleterious for enzyme function or that single amino acid mutations alone might not sufficiently decrease affinity of this putative inhibitor. The upregulation of *ndhA* could serve to compensate for loss of NDH-2 function or could serve to bind excess inhibitor in the cell. It is intriguing that *ndh* promoter mutations were not identified possibly because this gene is not readily upregulated by single nucleotide substitutions in its promoter. We also identified mutations in *Rv0678* (Table S1) encoding a transcriptional repressor that has previously been demonstrated to control expression of the MmpS5-MmpL5 transporter and has been implicated in resistance to bedaquiline and clofazimine<sup>34</sup>. In accordance with the predicted essential role of NDH-2 as complex I in oxidative phosphorylation<sup>16</sup>, treatment of *MTb* with compound **1** resulted in depletion of cellular ATP levels, a phenomenon also observed with bedaquiline (TM207), an inhibitor of the ATP synthase, as well as EU306, an inhibitor of the cytochrome *bc*<sub>1</sub> complex<sup>35</sup> but not with inhibitors of macromolecular biosynthesis including INH (cell wall), Rif (RNA polymerase), and Kan (protein synthesis)(Figure 3).

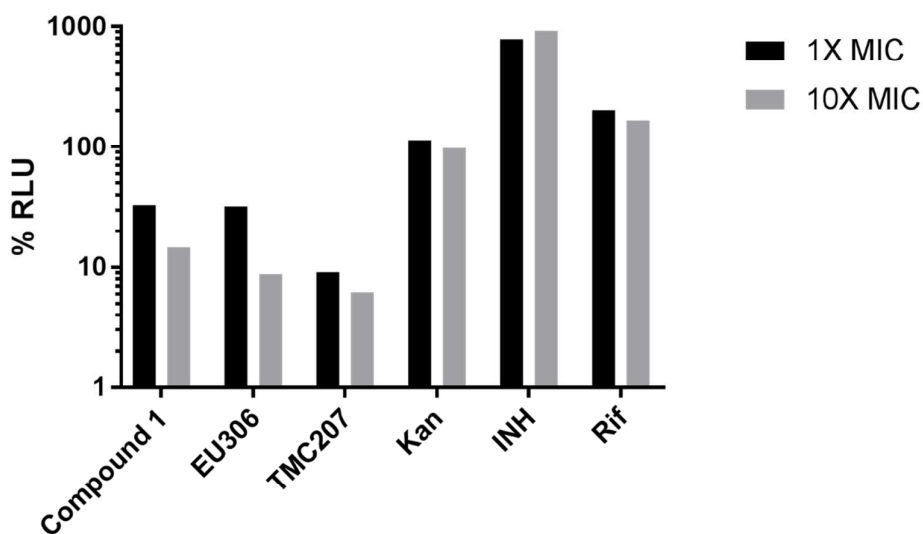


**Figure 3. Mercapto-quinazolinones deplete cellular ATP levels in *MTb*.** ATP was measured using the BacTiter Glo assay after 24 hours of drug exposure and expressed as a fraction of the drug-free vehicle control levels.

We predicted that inhibition of NDH-2 would result in a more severe phenotype on a mutant lacking the second copy of the type II NADH dehydrogenase. Indeed, while treatment of wild-type *MTb* H37Rv at MIC concentrations could not fully suppress growth of cells over 7 days of treatment, similar concentrations of compound resulted in an almost 2-log kill of a  $\Delta ndhA$  mutant (Figure 4). Despite the higher vulnerability of the *ndhA* mutant to killing by compound **1**, the MIC to this strain as well as a *nuoG* deletion mutant lacking a functional type I NADH dehydrogenase, was indistinguishable from WT cells (results not shown). Inhibition of anaerobic non-replicating cells with compound **1** did not affect viability (Figure S6) which contrasts with the anaerobic cidal activity of other NDH-2 inhibitors including the phenothiazines<sup>16</sup> and a recently described quinolone scaffold<sup>19</sup>, possibly due to differences in compound access to the target under anaerobic conditions or to growth dependent differences in compound modification by *MTb*. In addition, this compound lacked activity against *MTb* growing in infected macrophages (Figure S7) possibly due GSH-catalysed compound inactivation or inability to access the mycobacterial phagosome.

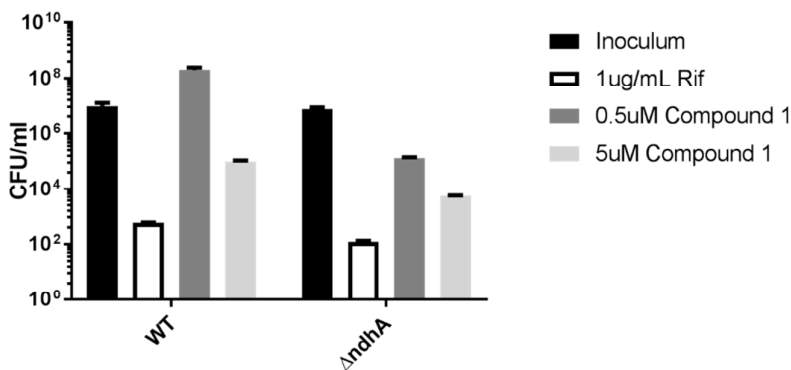


**Figure 4. *Mtb* lacking the alternative type II NADH dehydrogenase encoded by *ndhA* was more susceptible to compound **1**.** CFU after 7 days of treatment as compared to CFU at start of drug treatment



(inoculum). Unpaired t test comparison between WT and  $\Delta ndhA$  at 0.5  $\mu$ M compound **1**: two-tailed P value = 0.0023.

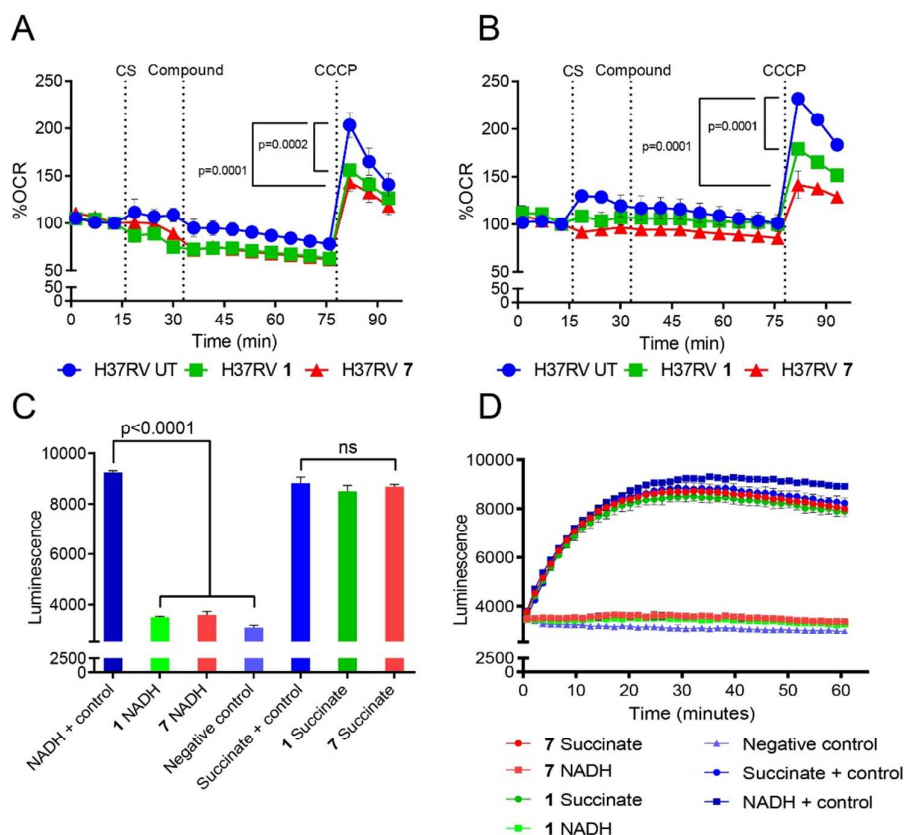


**Figure 5. Mercapto-quinazolinones target Complex I of the *MTb* ETC.** At the times indicated by the dotted vertical lines, either glucose (**A**) or palmitate (**B**) was added to *MTb* as carbon source (CS), followed by the mercapto-quinazolinones (Compound) and lastly, the uncoupler CCCP to induce maximal respiration. The mercapto-quinazolinones diminished *MTb*'s uncoupling capacity significantly compared to that of the untreated (UT) control. The oxygen consumption rate (OCR) is reported as a percentage of baseline values. Mercapto-quinazolinones inhibit ATP production in the presence of NADH, but not succinate (**C**, **D**). ATP production in inverted membrane vesicles (IMVs) in the presence of NADH or succinate as electron donors after 30 mins (**C**) and over 60 mins (**D**). *P*-values were calculated by one-way ANOVA using GraphPad Prism 7.02.

The effect of the mercapto-quinazolinones on *MTb* bioenergetics in whole cells was further demonstrated by analysis of the mycobacterial oxygen consumption rate (OCR) (Figure 5). Addition of compounds **1** and **7** had a minimal effect on basal *MTb* OCR levels over ~45 min. The same results were obtained in the presence of glucose or palmitate as carbon sources (Figure 5A and B). Uncoupling of *MTb* oxidative phosphorylation (OXPHOS) with carbonyl cyanide *m*-chlorophenyl hydrazone (CCCP) significantly diminished maximal respiration in the presence of the two inhibitors compared to the untreated control. These findings suggest an energy generation pathway common to both fatty acid and glucose oxidation as the target of the compounds. Previous studies<sup>21, 36</sup> have shown that *MTb* can rapidly reroute electron flux to overcome inhibition of cytochrome *bc*<sub>1</sub>-*aa*<sub>3</sub>, cytochrome *bd*, or ATP synthase, resulting in enhanced respiration. Therefore, we speculated that the target of compounds **1** and **7** was at the point of entry into the ETC - that is, Complex I (NADH dehydrogenase) or Complex II (succinate dehydrogenase). To test this prediction, ATP production was measured in *MTb* inverted membrane vesicles (IMVs) in the presence of the mercapto-quinazolinones (Figure 5C and D). Notably, ATP production was significantly inhibited when NADH was provided as electron donor but not when succinate was the source of reducing equivalents, suggesting that the site of inhibition was NADH dehydrogenase. The mechanism by which the compounds interfere with NADH dehydrogenase function differs from clofazimine and the quinolinequinones, which have been proposed to interfere with electron transport by activating NDH-2 resulting in production of reactive oxygen species<sup>18, 20</sup>.

To verify that NDH-2 was indeed the target for this class of mercapto-quinazolinones, we expressed *MTb* NDH-2 (MtNdh) encoded by the predicted essential *ndh* in *E. coli* as a recombinant MBP-fusion protein, and purified the protein to near homogeneity via amylose-resin affinity chromatography and gel filtration. The recombinant enzyme was highly active with coenzyme Q2 (ubiquinone Q-2) and NADH as substrates, delivering steady-state kinetic parameters similar to previously published results<sup>37</sup>. Quinazolinones **1-3**, **7** and **11** were found to have sub-micromolar IC<sub>50</sub> values against the MtNdh (Figure 6). Compounds **1**, **7**, and **11** showed the highest potency, with IC<sub>50</sub> values from 7-26 nM; values 3-orders of magnitude lower than that for the previously characterised NDH-2 inhibitor chlorpromazine (CPZ; 10-25 μM; Figure 6)<sup>24</sup> but

superior to the quinolonyl pyrimidines discovered in a target-based screening effort against the *MTb* NDH-2<sup>38</sup>. No time-dependent inhibition was observed for these compounds. The mode of inhibition against MtNdh was further investigated using compound **1**: double reciprocal plots of enzyme activity under varying concentrations of **1** and either Q2 or NADH suggested patterns indicative of a non-competitive mode of inhibition with both substrates ( $K_i$  values 30-40 nM), although the effect on slope was less evident when varying Q2 (Figure 7). This is similar to previous studies with a thiophenazine-based NDH-2 inhibitor<sup>39</sup>, and suggests that inhibition occurs through binding of the compound at an allosteric site, independent of the main substrate binding pockets.

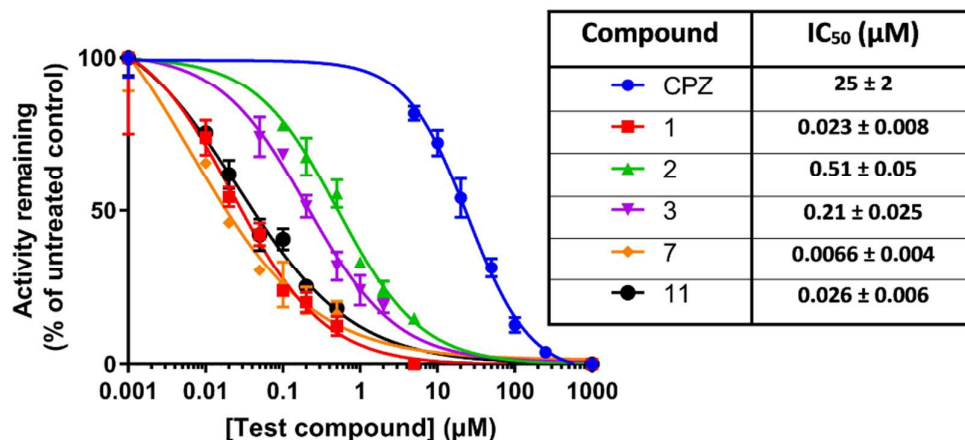


**Figure 6. Inhibition of recombinant MBP-MtNdh by select quinazolinones.** Steady-state enzyme activity was measured by monitoring absorbance changes at 340 nm due to NADH oxidation, as described in Materials and Methods. NADH and Q2 were fixed at 250 μM and 40 μM, respectively. Each data point is the mean ± SD of at least 3 independent measurements. Inset table shows calculated IC<sub>50</sub> values.

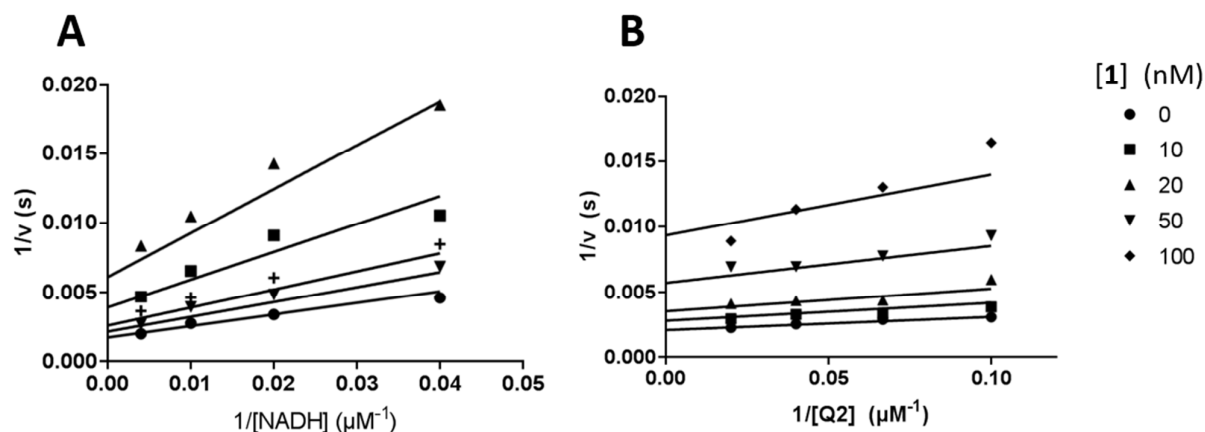


**Figure 7. Double-reciprocal plot of inhibition kinetics of MBP-MtNdh by 1.** NADH (left) or Q2 (right) concentrations were varied, in the presence of fixed concentrations of 40  $\mu\text{M}$  Q2 (A) or 250  $\mu\text{M}$  NADH (B). Data points are the average of at least 3 independent measurements. Solid lines represent best-fit values of the data to the general Michaelis-Menten reversible inhibition equation, using non-linear regression analysis.

In conclusion, the non-proton pumping type II NADH dehydrogenase (NDH-2) has been shown to play a critical role in the respiratory metabolism of bacteria. The 2-mercapto-quinazolinone scaffold is a potent inhibitor of the mycobacterial NDH-2 and although in this study *MTb* whole-cell SAR only obtained limited improvement in potency, this information, together with the recently disclosed structural information of the enzyme from the bacterium *Caldalkalibacillus thermarum*<sup>40</sup>, will aid in the future rational structure based development of new and improved NDH-2 inhibitors. Critical for any structure-guided inhibitor design is an understanding of the ligand-binding pocket of the NDH-2 protein. The low amino acid identity between the *C. thermarum* and *MTb* NDH-2 proteins (30%) combined with the finding that this inhibitor likely binds to an allosteric site with no allosteric ligand-binding sites identified on the existing bacterial NDH-2 structure<sup>40</sup>, suggests that co-crystallization of the compound with the *MTb* NDH-2 protein will be essential to facilitate rational drug design. During revision of this paper, the SAR of a similar mercapto-quinazolinone scaffold<sup>41</sup> was reported with a complementary paper describing the importance of the mycobacterial type II NADH dehydrogenase despite the non-essentiality of the individual *ndh* and *ndhA* genes<sup>42</sup>.

## EXPERIMENTAL

*Chemistry summary:* All commercially available reagents, solvents and starting materials were purchased from Aldrich Chemical Co. (UK). Where necessary a Biotage FLASH 25+ column chromatography system was used to purify mixtures; reagent-grade solvents used for chromatography were purchased from Fisher Scientific (UK) and flash column chromatography silica cartridges were obtained from Biotage (UK). Analytical thin-layer chromatography (TLC) was performed on precoated TLC plates (layer 0.20 mm silica gel 60 with fluorescent indicator UV254, from Merck). Developed plates were air-dried and analyzed under a UV lamp (UV 254/365 nm). Microwave irradiation was conducted using a BIOTAGE<sup>®</sup> INITIATOR unit. The machine consists of a continuous focused microwave power delivery system with operator-selectable power output (0-400 W at 2.45 GHz). All <sup>1</sup>H and <sup>13</sup>C NMR spectra were recorded on a Bruker ARX-500 spectrometer (500 and 300 MHz for <sup>1</sup>H and <sup>13</sup>C NMR, respectively). Chemical shifts ( $\delta$ ) are reported in ppm relative to the residual solvent peak or internal standard (tetramethylsilane), and coupling constants (*J*) are reported in hertz (Hz). Data are reported as follows: chemical shift, multiplicity (br=broad, s=singlet, d=doublet, t=triplet, m=multiplet), integration. LC–MS analyses were performed with either an Agilent HPLC 1100 series connected to a Bruker Daltonics MicroTOF or an Agilent Technologies 1200 series HPLC connected to an Agilent Technologies 6130 quadrupole spectrometer, where both instruments were connected to an Agilent diode array detector. LC–MS chromatographic separations were conducted with a Waters X bridge C18 column, 50 mm  $\times$  2.1 mm, 3.5  $\mu$ m particle size; mobile phase, water/acetonitrile + 0.1% HCOOH, or water/acetonitrile + 0.1% NH<sub>3</sub>; linear gradient from 80:20 to 5:95 over 3.5 min and then held for 1.5 min; flow rate of 0.5 mL.min<sup>-1</sup>. All assay compounds had a measured purity of  $\geq$ 95% (by TIC and UV) as determined using this analytical LC–MS system. High resolution electrospray measurements were performed on a Bruker Daltonics MicroTOF mass spectrometer.

**General method for the preparation of amide coupling (1, 4-11, 14-16, 19-27)** To a solution of 2-((4-oxo-3,4-dihydroquinazolin-2-yl)thio)acetic acid (1.0 equ) in a 1:1 ratio of acetonitrile (1.5 mL) and DMF (1.5 mL) were added EDC.HCl (1.0 equ), HOAT (1.2 equ) or HATU (1.0 equ), and primary/secondary amine (1.0 equ)

1  
2  
3 stirred for 30 min, DIPEA (2.0 equ) was added to the reaction mixture and stirred at room temperature  
4  
5 overnight. If a precipitate had formed this was filtered off, washed with acetonitrile and air dried. If the  
6  
7 reaction mixture had remained homogenous the solution was purified directly by preparative HPLC under  
8  
9 acidic conditions, using 0.1 % HCOOH in water:acetonitrile (5-95%) gradient elution to afford the product.

10  
11  
12  
13 **N-Cyclohexyl-2-((4-oxo-3,4-dihydroquinazolin-2-yl)thio)acetamide (1).** To a solution of acid of 2-((4-oxo-  
14  
15 3,4-dihydroquinazolin-2-yl)thio)acetic acid (**30**) (500 mg, 2.1 mmol, 1.0 equ) in 1:1 ratio of acetonitrile (1.5  
16  
17 mL) and DMF (1.5 mL) were added EDC.HCl (1.2 equ), HOAT (1.2 equ) or HATU (804 mg, 2.1 mmol, 1.0 equ)  
18  
19 in DCM (3 mL) and Cyclohexylamine (209 mg, 2.1 mmol, 1.0 equ) stirred for 30 min, DIPEA (0.73 mL, 2.1  
20  
21 mmol, 2.0 equ) was added to the reaction mixture and stirred at room temperature overnight. The reaction  
22  
23 mixture was purified by preparative HPLC under acidic conditions, using 0.1% HCOOH in water:acetonitrile  
24  
25 (5-95%) gradient elution to afford a white solid of N-cyclohexyl-2-((4-oxo-3,4-dihydroquinazolin-2-  
26  
27 yl)thio)acetamide as a white powder (450 mg, 66% yield),  $C_{16}H_{19}N_3O_2S$ , MW 317.41;  $^1H$  NMR (500 MHz,  
28  
29 DMSO)  $\delta$  12.66 (brs, 1H), 8.14 (d,  $J=7.9$  Hz, 1H), 8.04 (dd,  $J=1.3, 7.9$  Hz, 1H), 7.80 - 7.76 (m, 1H), 7.50 (d,  $J=$   
30  
31 7.9 Hz, 1H), 7.45 - 7.41 (m, 1H), 3.92 (s, 2H), 3.59 - 3.51 (m, 1H), 1.76 - 1.64 (m, 4H), 1.55 (dd,  $J=3.5, 9.1$  Hz,  
32  
33 1H), 1.30 - 1.12 (m, 5H). LCMS  $m/z$  318.12  $[M+1]^+$  100%. HRMS ( $m/z$ ):  $[M + H]^+$  calcd for  $C_{16}H_{20}N_3O_2S$ ,  
34  
35 318.1270; found 318.1284.

36  
37  
38  
39  
40  
41 **N-Cycloheptyl-2-((4-oxo-3,4-dihydroquinazolin-2-yl)thio)acetamide (4).** White powder (21 mg, 23% yield),  
42  
43  $C_{17}H_{21}N_3O_2S$ , MW 331.43;  $^1H$  NMR (500 MHz, DMSO)  $\delta$  12.65 (brs, 1H), 8.26 (d,  $J=7.8$  Hz, 1H), 8.02 (dd,  $J=$   
44  
45 1.3, 7.9 Hz, 1H), 7.77 - 7.72 (m, 1H), 7.48 - 7.37 (m, 2H), 3.88 (s, 2H), 3.73 (ddd,  $J=4.2, 8.6, 16.9$  Hz, 1H),  
46  
47 1.60 - 1.34 (m, 12H). LCMS  $m/z$  332.14  $[M+1]^+$  100%. HRMS ( $m/z$ ):  $[M + H]^+$  calcd for  $C_{17}H_{22}N_3O_2S$ , 332.1427;  
48  
49 found 332.1439.

50  
51  
52  
53 **N-Cyclopentyl-2-((4-oxo-3,4-dihydroquinazolin-2-yl)thio)acetamide (5).** White powder (39 mg, 24% yield),  
54  
55  $C_{15}H_{17}N_3O_2S$ , MW 303.38;  $^1H$  NMR (500 MHz, DMSO)  $\delta$  8.23 (d,  $J=7.1$  Hz, 1H), 8.04 (dd,  $J=1.3, 8.0$  Hz, 1H),  
56  
57 7.79 - 7.75 (m, 1H), 7.49 (d,  $J=8.0$  Hz, 1H), 7.45 - 7.41 (m, 1H), 4.03 - 3.98 (m, 1H), 3.91 (s, 2H), 1.82 - 1.76  
58  
59

(m, 2H), 1.67 - 1.62 (m, 2H), 1.53 - 1.36 (m, 4H). LCMS  $m/z$  304.12  $[M + H]^+$  100%. HRMS ( $m/z$ ):  $[M + H]^+$  calcd for  $C_{15}H_{18}N_3O_2S$ , 304.1114; found 304.1107.

**N-Cyclobutyl-2-((4-oxo-3,4-dihydroquinazolin-2-yl)thio)acetamide (6).** White powder (76 mg, 66% yield),  $C_{14}H_{15}N_3O_2S$ , MW 289.35;  $^1H$  NMR (400 MHz, DMSO)  $\delta$  12.67 (s, 1H), 8.54 (d,  $J$  = 7.7 Hz, 1H), 8.05 - 8.02 (m, 1H), 7.81 - 7.75 (m, 1H), 7.51 (d,  $J$  = 8.1 Hz, 1H), 7.43 (t,  $J$  = 7.5 Hz, 1H), 4.19 (dd,  $J$  = 8.1, 16.1 Hz, 1H), 3.91 (s, 2H), 2.20 - 2.10 (m, 2H), 1.97 - 1.85 (m, 2H), 1.67 - 1.57 (m, 2H). LCMS  $m/z$  290.04  $[M + H]^+$  100%. HRMS ( $m/z$ ):  $[M + H]^+$  calcd for  $C_{14}H_{16}N_3O_2S$ , 290.0957; found 290.0962.

**N-(4,4-Difluorocyclohexyl)-2-((4-oxo-3,4-dihydroquinazolin-2-yl)thio)acetamide (7).** To a solution of 2-((4-oxo-3,4-dihydroquinazolin-2-yl)thio)acetic acid **30** (108 mg, 0.4 mmol, 1.0 equ) in DCM (3 mL) were added HATU (160 mg, 0.4 mmol, 1.0 equ) and 4,4-difluorocyclohexan-1-amine (57 mg, 0.4 mmol, 1.0 equ) and stirred for 30 min, DIPEA (0.074 mL, 0.4 mmol, 2.0 equ) was added to the reaction mixture and stirred at room temperature overnight. The reaction mixture was purified by preparative HPLC under acidic conditions, using 0.1% HCOOH in water:acetonitrile (5-95%) gradient elution to afford a white solid of *N*-(4,4-difluorocyclohexyl)-2-((4-oxo-3,4-dihydroquinazolin-2-yl)thio)acetamide as a white powder **7** (115 mg, 75% yield),  $C_{16}H_{17}F_2N_3O_2S$ , MW 353.39;  $^1H$  NMR (500 MHz, DMSO)  $\delta$  12.64 (s, 1H), 8.39 (d,  $J$  = 6.9 Hz, 1H), 8.02 (dd,  $J$  = 1.2, 7.9 Hz, 1H), 7.77-7.72 (m, 1H), 7.46 (d,  $J$  = 7.9 Hz, 1H), 7.40 (t,  $J$  = 7.5 Hz, 1H), 3.90 (s, 2H), 3.77 (t,  $J$  = 4.0 Hz, 1H), 2.04 - 1.75 (m, 6H), 1.56 - 1.47 (m, 2H). LCMS  $m/z$  354.14  $[M + H]^+$  100%. HRMS ( $m/z$ ):  $[M + H]^+$  calcd for  $C_{16}H_{18}F_2N_3O_2S$ , 354.1082; found 354.1091.

**N-(4,4-Difluorocyclohexyl)-2-((4-oxo-3,4-dihydroquinazolin-2-yl)thio)acetamide HCl Salt preparation (7).** *N*-(4,4-difluorocyclohexyl)-2-((4-oxo-3,4-dihydroquinazolin-2-yl)thio)acetamide (60 mg, 0.17 mmol, 1.0 equ) in ethyl acetate (10 mL) and ethanol (3 mL) was heated up to 80°C, until dissolved (90%). The solution was cooled immediately, followed by the addition of 2M HCl in diethyl ether (1 mL, 747 mg, 20.49 mmol, 120 equ) and stirred for a further 15 min, where white precipitates were formed. The precipitate was filtered and dried to afford the *N*-(4,4-difluorocyclohexyl)-2-((4-oxo-3,4-dihydroquinazolin-2-

yl)thio)acetamide HCl Salt (50 mg, 75% yield),  $C_{16}H_{17}F_2N_3O_2S \cdot HCl$ , MW 389.85;  $^1H$  NMR (500 MHz, DMSO)  $\delta$  8.32 (d,  $J = 7.6$  Hz, 1H), 8.04 (dd,  $J = 1.2, 7.9$  Hz, 1H), 7.80-7.76 (m, 1H), 7.49 (d,  $J = 7.8$  Hz, 1H), 7.45-7.41 (m, 1H), 3.95 (s, 2H), 2.52-2.50 (m, 1H), 2.05 - 1.99 (m, 2H), 1.97 - 1.76 (m, 4H), 1.57 - 1.48 (m, 2H). LCMS  $m/z$  354.14  $[M + H]^+$  100%. HRMS ( $m/z$ ):  $[M + H]^+$  calcd for  $C_{16}H_{18}F_2N_3O_2S$ , 354.1082; found 354.1091.

**N-(2,2-Difluorocyclohexyl)-2-((4-oxo-3,4-dihydroquinazolin-2-yl)thio)acetamide (8).** White powder (93 mg, 62% yield),  $C_{16}H_{17}F_2N_3O_3S_2$ , MW 353.39;  $^1H$  NMR (500 MHz, DMSO)  $\delta$  12.64 (s, 1H), 8.46 (d,  $J = 9.0$  Hz, 1H), 8.04 (d,  $J = 7.9$  Hz, 1H), 7.79 - 7.75 (m, 1H), 7.50 (d,  $J = 8.2$  Hz, 1H), 7.43 (dd,  $J = 7.5$  Hz, 1H), 4.03 - 4.01 (m, 3H), 2.08 - 2.03 (m, 1H), 1.86 - 1.63 (m, 4H), 1.49 - 1.38 (m, 3H). LCMS  $m/z$  354.10  $[M + H]^+$  100%. HRMS ( $m/z$ ):  $[M + H]^+$  calcd for  $C_{16}H_{18}F_2N_3O_3S_2$ , 354.1082; found 354.1094.

**N-(3,3-Difluorocyclohexyl)-2-((4-oxo-3,4-dihydroquinazolin-2-yl)thio)acetamide (9).** White powder (83 mg, 55% yield),  $C_{16}H_{17}F_2N_3O_3S_2$ , MW 353.39;  $^1H$  NMR (500 MHz, DMSO)  $\delta$  12.61 (brs, 1H), 8.31 (d,  $J = 7.9$  Hz, 1H), 8.04 (dd,  $J = 1.3, 7.9$  Hz, 1H), 7.80 - 7.76 (m, 1H), 7.50 (d,  $J = 8.2$  Hz, 1H), 7.43 (t,  $J = 7.5$  Hz, 1H), 3.94 (s, 2H), 3.91 - 3.75 (m, 1H), 2.21 - 2.15 (m, 1H), 1.98 - 1.95 (m, 1H), 1.81 - 1.68 (m, 4H), 1.45 - 1.24 (m, 2H). LCMS  $m/z$  354.10  $[M + H]^+$  100%. HRMS ( $m/z$ ):  $[M + H]^+$  calcd for  $C_{16}H_{18}F_2N_3O_3S_2$ , 354.1082; found 354.1095.

**N-(Cyclohexylmethyl)-2-((4-oxo-3,4-dihydroquinazolin-2-yl)thio)acetamide (10).** White powder (34 mg, 25% yield),  $C_{17}H_{21}N_3O_2S$ , MW 331.43;  $^1H$  NMR (500 MHz, DMSO)  $\delta$  12.64 (s, 1H), 8.16 (s, 1H), 8.05 - 8.02 (m, 1H), 7.79 - 7.75 (m, 1H), 7.50 (dd,  $J = 3.1, 8.1$  Hz, 1H), 7.44 - 7.40 (m, 1H), 3.93 (d,  $J = 2.5$  Hz, 2H), 2.95 - 2.92 (m, 2H), 1.67 - 1.58 (m, 5H), 1.38 - 1.34 (m, 1H), 1.12 - 1.07 (m, 3H), 0.87 - 0.79 (m, 2H). LCMS  $m/z$  332.21  $[M + H]^+$  100%. HRMS ( $m/z$ ):  $[M + H]^+$  calcd for  $C_{17}H_{22}N_3O_2S$ , 332.1427; found 332.1431.

**N-((4,4-Difluorocyclohexyl)methyl)-2-((4-oxo-3,4-dihydroquinazolin-2-yl)thio)acetamide (11).** White powder (120 mg, 77% yield),  $C_{17}H_{19}N_3F_2O_2S$ , MW 367.41;  $^1H$  NMR (500 MHz, DMSO)  $\delta$  12.64 (s, 1H), 8.27 (t,  $J = 5.8$  Hz, 1H), 8.04 (dd,  $J = 1.3, 7.9$  Hz, 1H), 7.80 - 7.76 (m, 1H), 7.50 (d,  $J = 8.0$  Hz, 1H), 7.45 - 7.42 (m, 1H), 3.95 (s, 2H), 3.02 (t,  $J = 6.4$  Hz, 2H), 1.96 - 1.87 (m, 2H), 1.74 - 1.52 (m, 5H),



1.17 - 1.08 (m, 2H). LCMS  $m/z$  368.01  $[M + H]^+$  100%. HRMS ( $m/z$ ):  $[M + H]^+$  calcd for  $C_{17}H_{20}N_3F_2O_2S$ , 368.1238; found 368.1255.

**N-Cyclohexyl-N-methyl-2-((4-oxo-3,4-dihydroquinazolin-2-yl)thio)acetamide (14).** White powder (35 mg, 25% yield),  $C_{17}H_{21}N_3O_2S$ , MW 331.43;  $^1H$  NMR (500 MHz, DMSO)  $\delta$  12.60 (brs, 1H), 8.04 (dd,  $J = 1.6, 7.9$  Hz, 1H), 7.80 - 7.74 (m, 1H), 7.49 - 7.40 (m, 2H), 4.34 (s, 1H), 4.23 (s, 1H), 3.80 - 3.76 (m, 1H), 3.01 (s, 2H), 2.74 (s, 1H), 1.76 (t,  $J = 12.0$  Hz, 3H), 1.62 - 1.52 (m, 2H), 1.52 - 1.43 (m, 2H), 1.38 - 1.23 (m, 2H), 1.15 - 1.05 (m, 1H). LCMS  $m/z$  332.15  $[M + H]^+$ . HRMS ( $m/z$ ):  $[M + H]^+$  calcd for  $C_{17}H_{22}N_3O_2S$ , 332.1427; found 332.1440.

**2-((4-Oxo-3,4-dihydroquinazolin-2-yl)thio)propanoic acid (56).** To a solution of 2-thioxo-2,3-dihydroquinazolin-4(1H)-one **29** (500 mg, 2.8 mmol, 1.0 equ), were added 2-bromopropanoic acid (557 mg, 3.6 mmol, 1.3 equ) and triethylamine (2.3 mL, 16.8 mmol, 6.0 equ) in DMF (5 mL), and stirred for 12 hr at 75°C. Once the reaction has completed, it was poured onto crushed ice and acidified with 1N HCl, where the product precipitated out of the solution. The precipitate was filtered and dried to yield 2-((4-oxo-3,4-dihydroquinazolin-2-yl)thio)propanoic acid **56** (548 mg, 78% yield),  $C_{11}H_{10}N_2O_3S$ , MW 250.27;  $^1H$  NMR (500 MHz, DMSO)  $\delta$  12.66 (s, 1H), 8.04 (q,  $J = 3.10$  Hz, 1H), 7.70 (m, 1H), 7.50 (d,  $J = 8.00$  Hz, 1H), 7.44 (m, 1H), 4.57 (q,  $J = 7.3$  Hz, 2H), 1.55 (d,  $J = 7.30$  Hz, 3H). LCMS  $m/z$  251.00  $[M + H]^+$  100%.

**N-Cyclohexyl-2-((4-oxo-3,4-dihydroquinazolin-2-yl)thio)propanamide (15).** White powder (45 mg, 35% yield),  $C_{17}H_{21}N_3O_2S$ , MW 331.43;  $^1H$  NMR (500 MHz, DMSO)  $\delta$  12.59 (brs, 1H), 8.17 (d,  $J = 7.7$  Hz, 1H), 8.04 (dd,  $J = 1.4, 7.9$  Hz, 1H), 7.81 - 7.77 (m, 1H), 7.53 (d,  $J = 8.2$  Hz, 1H), 7.45 - 7.42 (m, 1H), 4.54 (q,  $J = 7.0$  Hz, 1H), 3.56 - 3.48 (m, 1H), 1.76 - 1.61 (m, 4H), 1.53 - 1.50 (m, 4H), 1.29 - 1.10 (m, 5H). LCMS  $m/z$  332.10  $[M + H]^+$  100%. HRMS ( $m/z$ ):  $[M + H]^+$  calcd for  $C_{17}H_{22}N_3O_2S$ , 332.1427; found 332.1432.

**N-Cyclohexyl-N-methyl-2-((4-oxo-3,4-dihydroquinazolin-2-yl)thio)propanamide (16).** White powder (40 mg, 29% yield),  $C_{18}H_{23}N_3O_2S$ , MW 345.46;  $^1H$  NMR (500 MHz, DMSO)  $\delta$  12.60 (brs, 1H), 8.07 - 8.02 (m, 1H), 7.82 - 7.75 (m, 1H), 7.50 - 7.41 (m, 2H), 4.24 - 4.18 (m, 1H), 3.05 (s, 2H), 2.75 (s, 1H), 1.80 - 1.70 (m, 3H),

1.64 - 1.54 (m, 1H), 1.54 - 1.47 (m, 6H), 1.36 - 1.20 (m, 2H), 1.14 - 1.02 (m, 2H). LCMS  $m/z$  346.10  $[M + H]^+$  100%. HRMS ( $m/z$ ):  $[M + H]^+$  calcd for  $C_{18}H_{24}N_3O_2S$ , 346.1584; found 346.1608.

**N-Cyclohexylglycine (53).** Cyclohexylamine **51** (100 mg, 1.0 mmol, 1.0 equ) and ethyl 2-hydroxyacetate **52** (104.9 mg, 1.0 mmol, 61.0 equ) were stirred neat in a round-bottom flask for 12 h. The solvent of the crude mixture was evaporated completely, and the residue purified via flash column chromatography eluting with 10% DCM in methanol to afford N-Cyclohexylglycine **53** (100 mg, 63% yield),  $C_8H_{15}NO_2$ , MW 157.21 ;  $^1H$  NMR (500 MHz, DMSO)  $\delta$  6.34 (brs, 1H), 4.05 – 4.04 (m, 2H), 3.82 – 3.77 (m, 1H), 3.77-3.69 (m, 1H), 1.86-1.83 (q,  $J$  = 5.28 Hz, 2H), 1.67-1.63 (m, 2H), 1.57-1.53 (m, 1H), 1.35-1.26 (m, 2H), 1.15-1.07 (m, 3H). LCMS  $m/z$  158.21  $[M + H]^+$  100%.

**2-(Methylthio)quinazolin-4(3H)-one (54).** A solution of iodomethane (398 mg, 2.8 mmol, 1.0 equ) in methanol (8 mL) was added slowly to a closed vessel containing a solution of 2-thioxo-2,3-dihydroquinazolin-4(1H)-one **29** (500 mg, 2.8 mmol, 1.0 equ) in 1% aqueous NaOH (8 mL) under  $N_2$  atmosphere and stirred for 1 h at room temperature. The reaction mixture was then cooled to 0°C, and the pH adjusted to 7 with an aqueous solution of 1N HCl. The solvent was removed under reduced pressure, and the solid was filtered, washed with water/methanol and dried to afford 2-(methylthio)quinazolin-4(3H)-one **54** (532 mg, 98% yield),  $C_9H_8N_2OS$ , MW 192.24;  $^1H$  NMR (500 MHz, DMSO)  $\delta$  12.62 (s, 1H), 8.09 (q,  $J$  = 3.13 Hz, 1H), 7.81 (m, 1H), 7.59 (d,  $J$  = 8.10 Hz, 1H), 7.47 (m, 1H), 2.63 (s, 3H). LCMS  $m/z$  193.18  $[M + H]^+$  100%.

**N-Cyclohexyl-2-((4-oxo-3,4-dihydroquinazolin-2-yl)amino)acetamide (17).** 2-amino-N-cyclohexylacetamide **55** (40.63 mg, 0.26 mmol, 1.0 equ), 2-(methylthio)quinazolin-4(3H)-one **54** (50 mg, 0.26 mmol, 1.0 equ) were suspended in ethyl acetate (2 mL) in a sealed microwave vial and irradiated (0-400 W at 2.65 Ghz) at 140°C for 2 h. Upon completion the reaction was filtered and the filtrate was extracted with diethyl ether to afford N-Cyclohexyl-2-((4-oxo-3,4-dihydroquinazolin-2-yl)amino)acetamide as a white powder **17** (4.4 mg, 4.4% yield),  $C_{16}H_{20}N_4O_2$ , MW 300.36;  $^1H$  NMR (500 MHz, DMSO)  $\delta$  8.10 (d,  $J$  = 7.7 Hz, 1H), 7.58 -

7.56 (m, 1H), 7.33 (d,  $J = 8.7$  Hz, 1H), 7.22 - 7.18 (m, 1H), 3.95 (s, 2H), 1.76-1.66 (m, 4H), 1.56 - 1.53 (m, 1H), 1.31 - 1.07 (m, 6H). LCMS  $m/z$  301.0  $[M + H]^+$  100%. HRMS ( $m/z$ ):  $[M + H]^+$  calcd for  $C_{16}H_{21}N_4O_2$ , 301.1659; found 301.1665.

**N-Cyclohexyl-2-((4-oxo-3,4-dihydroquinazolin-2-yl)oxy)acetamide (18).** 2-(methylthio)quinazolin-4(3H)-one **54** (50 mg, 0.26 mmol, 1.0 equ) and N-cyclohexylglycine **53** (21.7 mg, 0.12 mmol, 1.0 equ) were dissolved in THF (2 mL) and heated to 80 °C. Upon reaction completion the crude product was directly purified via prep-HPLC Gilson purification using 0.1% ammonia in water:acetonitrile 5-95% gradient elution to afford the product as a white powder **18** (10 mg, 24% yield),  $C_{16}H_{19}N_3O_3$ , MW 301.34;  $^1H$  NMR (500 MHz, DMSO)  $\delta$  12.36 (brs, 1H), 8.03 (d,  $J = 7.7$  Hz, 1H), 7.9 (d, 1H), 7.73 (d,  $J = 8.7$  Hz, 1H), 7.40-7.33 (m, 1H), 3.77 (s, 2H), 3.60 - 3.56 (m, 1H), 1.76-1.66 (m, 4H), 1.57-1.53 (m, 1H), 1.31 - 1.10 (m, 6H). LCMS  $m/z$  302.1  $[M + H]^+$  100%. HRMS ( $m/z$ ):  $[M + H]^+$  calcd for  $C_{16}H_{20}N_3O_{3.2}$ , 302.1499; found 302.1487.

**N-Cyclohexyl-3-(4-oxo-3,4-dihydroquinazolin-2-yl)propanamide (19).** White powder (110 mg, 80% yield),  $C_{17}H_{21}N_3O_2$ , MW 299.37;  $^1H$  NMR (500 MHz, DMSO)  $\delta$  12.18 (s, 1H), 8.08 (dd,  $J = 1.3, 7.9$  Hz, 1H), 7.85 - 7.76 (m, 2H), 7.56 (d,  $J = 8.0$  Hz, 1H), 7.48 - 7.45 (m, 1H), 3.55 - 3.48 (m, 1H), 2.83 (t,  $J = 7.4$  Hz, 2H), 2.58 (t,  $J = 7.4$  Hz, 2H), 1.73 - 1.64 (m, 4H), 1.55 - 1.52 (m, 1H), 1.28 - 1.09 (m, 5H). LCMS  $m/z$  300.10  $[M + H]^+$  100%. HRMS ( $m/z$ ):  $[M + H]^+$  calcd for  $C_{17}H_{22}N_3O_2$ , 300.1707; found 300.1721.

**2-((3-Methyl-4-oxo-3,4-dihydroquinazolin-2-yl)thio)acetic acid (50).** 2-mercapto-3-methylquinazolin-4(3H)-one **49** (220 mg, 1.14 mmol, 1.0 equ), 2-bromoacetic acid (206 mg, 1.48 mmol, 1.3 equ) and triethylamine (0.95 mL, 6.8 mmol, 6.0 equ) were stirred in DMF (5 mL) for 12 hr at 75° C. Upon reaction completion the reaction mixture was poured onto crushed ice, acidified with 1N HCl. The precipitate formed was collected and dried to afford the product 2-((3-Methyl-4-oxo-3,4-dihydroquinazolin-2-yl)thio)acetic acid **50** (250 mg, 87% yield), as a white powder.  $C_{11}H_{10}N_2O_3S$ , MW 250.27;  $^1H$  NMR (500 MHz, DMSO)  $\delta$  12.89 (s, 1H), 8.08 (q,  $J = 3.05$  Hz, 1H), 7.79 (m, 1H), 7.46 (m, 2H), 4.11 (s, 2H), 3.55 (s, 3H). LCMS  $m/z$  251.04  $[M + H]^+$  100%.

**N-Cyclohexyl-2-((3-methyl-4-oxo-3,4-dihydroquinazolin-2-yl)thio)acetamide (20).** White powder (20 mg, 15% yield),  $C_{17}H_{21}N_3O_2S$ , MW 331.42;  $^1H$  NMR (500 MHz, DMSO)  $\delta$  8.15 (d,  $J$  = 7.9 Hz, 1H), 8.08 (d,  $J$  = 7.9 Hz, 1H), 7.82 - 7.78 (m, 1H), 7.52 (d,  $J$  = 8.2 Hz, 1H), 7.47 - 7.43 (m, 1H), 3.98 (s, 2H), 3.54 (s, 4H), 1.76 - 1.65 (m, 4H), 1.55 (d,  $J$  = 12.8 Hz, 1H), 1.28 - 1.11 (m, 5H). LCMS  $m/z$  332.15  $[M + H]^+$  100%. HRMS ( $m/z$ ):  $[M + H]^+$  calcd for  $C_{17}H_{22}N_3O_2S$ , 332.1427; found 332.1436.

**2-(Quinazolin-2-ylthio)acetic acid (44).** 2-chloroquinazoline **43** (0.2 g, 1.22 mmol) and sodium thioglycolic acid **39b** (1 equiv) were dissolved in DMF and triethylamine (6.0 equiv) added. The reaction mixture was heated to 100°C overnight. The resulting precipitate was filtered and used without any further purification to afford the product 2-(Quinazolin-2-ylthio)acetic acid **44** (0.153 g, 57% yield) as a white powder.  $C_{10}H_8N_2O_2S$ , MW 220.25,  $^1H$  NMR (500 MHz, DMSO)  $\delta$  9.41 (d,  $J$  = 1.5 Hz, 1H), 8.09 (m, 1H), 7.95-7.93 (m, 1H), 7.79-7.77 (m, 1H), 7.66-7.61 (m, 1H), 4.05 (s, 2H). LCMS  $m/z$  221.1  $[M + H]^+$  100%.

**N-Cyclohexyl-2-(quinazolin-2-ylthio)acetamide (21).** White powder (21 mg, 10% yield),  $C_{16}H_{19}N_3OS$ , MW 301.41;  $^1H$  NMR (300 MHz, DMSO)  $\delta$  9.36 (m, 1H), 8.05-8.0 (m, 2H), 7.79-7.76 (m, 1H), 3.95 (s, 2H), 3.52-3.48 (m, 1H), 2.49-2.48 (m, 2H), 1.72-1.32 (m, 5H), 1.25-1.21 (m, 3H). LCMS  $m/z$  302.1  $[M + H]^+$  100%.

**2-((4-Aminoquinazolin-2-yl)thio)acetic acid (46).** 2-Chloroquinazolin-4-amine **45** (0.2 g, 1.11 mmol, 1.0 equ), sodium thioglycolic acid **39b** (0.103 g, 1.11 mmol, 1.0 equ) and triethylamine were dissolved in DMF (2ml) (0.93 ml, 6.68 mmol, 6.0 equ). The reaction mixture was heated to 100°C overnight. The resulting precipitate was filtered to afford a white powder (0.2 g, 76% yield), and used without further purification LCMS (ESI)  $m/z$  236.1  $[M + H]^+$

**2-((4-Aminoquinazolin-2-yl)thio)-N-cyclohexylacetamide (22).** White powder (21 mg, 10% yield),  $C_{16}H_{20}N_4OS$ , MW 316.42;  $^1H$  NMR (300 MHz, DMSO)  $\delta$  8.13 (dd,  $J$  = 3.0, 6.0 Hz, 1H), 7.97 (d,  $J$  = 6 Hz, 1H),

7.87 (brs, 2H), 7.77-7.69 (m, 1H), 7.51-7.49 (m, 1H), 7.38-7.34 (m, 1H), 3.75 (s, 2H), 3.55-3.45 (m, 1H), 1.76-1.47 (m, 5H), 1.23-1.09 (m, 5H). LCMS  $m/z$  317.1  $[M + H]^+$  100%.

**2-((4-Oxo-3,4,5,6,7,8-hexahydroquinazolin-2-yl)thio)acetic acid (40).** 2-sulfanyl-5,6,7,8-tetrahydro-4-quinazolinol **38** (0.1 g, 5.49 mmol, 1.0 equiv), chloroacetic acid **39a** (1.3 equiv.) and triethylamine (6 equiv.) were stirred in DMF at room temperature overnight. Once the reaction was complete, the reaction mixture was poured over crushed ice and acidified with 1N HCl. The white precipitate was collected by filtration and washed with water to afford the product as a white powder (750 mg, 58% yield) which was used without further purification.  $C_{10}H_{12}N_2O_3S$ , MW 240.28;  $^1H$  NMR (300 MHz, DMSO)  $\delta$  12.59 (brs, 1H), 3.93 (s, 2H), 2.45 (t,  $J = 3.0$  Hz, 2H), 2.29 (t,  $J = 3.0$  Hz, 2H), 1.70-1.63 (m, 4H). LCMS (ESI):  $m/z$  239.1  $[M - H]^+$  100%.

**N-Cyclohexyl-2-((4-oxo-3,4,5,6,7,8-hexahydroquinazolin-2-yl)thio)acetamide (23).** White powder (43 mg, 17% yield),  $C_{16}H_{23}N_3O_2S$ , MW 321.44;  $^1H$  NMR (300 MHz, DMSO)  $\delta$  12.47 (brs, 1H), 8.00 (brs, 1H), 3.80 (s, 2H), 3.58-3.49 (m, 1H), 2.47 (t,  $J = 3.0$  Hz, 2H), 2.31 (t,  $J = 3.0$  Hz, 2H), 1.75-1.54 (m, 9H), 1.29-1.13 (m, 5H). LCMS  $m/z$  320.1  $[M - H]^+$  100%.

**2-((4-Oxo-4,5,6,7-tetrahydro-3H-cyclopenta[d]pyrimidin-2-yl)thio)acetic acid (42).** 2-thioxo-1,2,3,5,6,7-hexahydro-4H-cyclopenta[d]pyrimidin-4-one **41** (1.0 g, 5.94 mmol, 1.0 equiv), chloroacetic acid **39a** (1.3 equiv.) and triethylamine (6 equiv.) were stirred in DMF (2 mL) at room temperature overnight. Once the reaction was complete it was poured over crushed ice and acidified with 1N HCl. The white precipitate was collected by filtration and washed with water to afford the product as a white powder (800 mg, 59% yield), which was used without further purification.  $C_9H_{10}N_2O_3S$ , MW 226.05;  $^1H$  NMR (300 MHz, DMSO)  $\delta$  12.65 (brs, 1H), 3.96 (s, 2H), 2.71 (t,  $J = 3.0$  Hz, 2H), 2.58 (t,  $J = 3.0$  Hz, 2H), 1.97-1.93 (m, 2H). LCMS  $m/z$  227.1  $[M + H]^+$  100%.

**N-Cyclohexyl-2-((4-oxo-4,5,6,7-tetrahydro-3H-cyclopenta[d]pyrimidin-2-yl)thio)acetamide(24).** White powder (59 mg, 22% yield),  $C_{15}H_{23}N_3O_2S$ , MW 307.41;  $^1H$  NMR (300 MHz, DMSO)  $\delta$  12.59 (brs, 1H), 8.03 (s,

1H), 3.84 (s, 2H), 3.58-3.49 (m, 1H), 2.71 (t,  $J = 3.0$  Hz, 2H), 2.60 (t,  $J = 3.0$  Hz, 2H), 2.0-1.92 (m, 2H), 1.75-1.52 (m, 5H), 1.29-1.16 (m, 5H). LCMS (ESI):  $m/z$  308.1  $[M + H]^+$  100%.

**2-((4,5-Dimethyl-6-oxo-1,6-dihydropyrimidin-2-yl)thio)acetic acid (48).** 5,6-Dimethyl-2-thiouracil **47** (0.5 g, 3.20 mmol), chloroacetic acid **39a** (0.39 g, 4.16 mmol) and triethylamine (2.62 mL, 1.94 mmol) were stirred in DMF (2 mL) at room temperature overnight. Once the reaction was complete, it was poured over crushed ice and acidified with 1N HCl. The white precipitate was collected by filtration and washed with water to afford the product as a white powder (0.36 g, 54% yield) which was used without further purification.  $C_8H_{10}N_2O_3S$ , MW 214.24,  $^1H$  NMR (300 MHz, DMSO)  $\delta$  12.56 (brs, 1H), 3.89 (s, 2H), 2.14 (s, 3H), 1.85 (s, 3H). LCMS (ESI):  $m/z$  213.1  $[M - H]$ ; HPLC purity 98%.

**N-Cyclohexyl-2-((4,5-dimethyl-6-oxo-1,6-dihydropyrimidin-2-yl)thio)acetamide (25).** White powder (0.047 g, 17% yield).  $C_{14}H_{21}N_3O_2S$ , MW 295.40;  $^1H$  NMR (400 MHz, DMSO- $d_6$ )  $\delta$  7.99 (dd,  $J = 20.3$ , 8.1 Hz, 1H), 3.80 (s, 2H), 3.11 – 2.97 (m, 1H), 2.20 (s, 3H), 1.89 (s, 3H), 1.78 – 1.64 (m, 5H), 1.33 – 1.12 (m, 5H). LCMS (ESI):  $m/z$  296.1  $[M + H]^+$  100%.

**6-Fluoro-2-thioxo-2,3-dihydroquinazolin-4(1H)-one (33).** 2-Amino-5-fluorobenzoic acid **32** (1 g, 6.5 mmol, 1.0 equ) and thiourea (2.1 g, 25.8 mmol, 6.0 equ) were heated neat in a round-bottom flask to 180°C for 3h with stirring. The reaction was cooled and 25 ml of water added. After stirring for 10 min the precipitate formed was filtered off, washed with cold water and dried to afford 6-Fluoro-2-thioxo-2,3-dihydroquinazolin-4(1H)-one **33** (0.45 g, 35.9% yield) as a yellow powder.  $C_8H_5FN_2OS$ , MW 196.2;  $^1H$  NMR (500 MHz, DMSO)  $\delta$  9.72 (s, 1H), 7.51-7.39 (m,  $J = 8.5$  Hz, 1H), 7.37-7.30 (m,  $J = 8.6$  Hz, 1H), 7.19-7.16 (m,  $J = 8.85$  Hz, 1H). LCMS  $m/z$  197.78  $[M + H]^+$  100%.

**2-((6-Fluoro-4-oxo-3,4-dihydroquinazolin-2-yl)thio)acetic acid (34).** 6-Fluoro-2-thioxo-2,3-dihydroquinazolin-4(1H)-one **33** (414 mg, 2.1 mmol, 1.0 equ), 2-bromoacetic acid (586.39 mg, 4.2 mmol, 2.0 equ) and triethylamine (1.76 mL, 12.6 mmol, 6.0 equ) were stirred in DMF (5 mL) at 75°C for 12 hr.

Upon reaction completion the reaction mixture was poured over crushed ice and acidified with 1N HCl. The precipitate was filtered and dried to afford 2-((6-Fluoro-4-oxo-3,4-dihydroquinazolin-2-yl)thio)acetic acid **34** (150 mg, 27.9% yield),  $C_{10}H_7FN_2O_3S$ , MW 254.24;  $^1H$  NMR (500 MHz, DMSO)  $\delta$  12.88 (s, 1H), 7.72 (q,  $J$  = 3.87 Hz, 1H), 7.65 (m, 1H), 7.54 (q,  $J$  = 4.62 Hz, 1H), 4.03 (s, 2H). LCMS  $m/z$  254.10  $[M + H]^+$  100%.

**N-(4,4-Difluorocyclohexyl)-2-((6-fluoro-4-oxo-3,4-dihydroquinazolin-2-yl)thio)acetamide (26).** To a solution of 2-((6-fluoro-4-oxo-3,4-dihydroquinazolin-2-yl)thio)acetic acid **34** (100 mg, 0.39 mmol, 1.0 equ) in a 1:1 ratio of acetonitrile (1.5 mL) and DMF (1.5 mL) were added EDC.HCl (90 mg, 0.74 mmol, 1.2 equ), HOAT (64 mg, 0.47 mmol, 1.2 equ) and 4,4-difluorocyclohexan-1-amine (67 mg, 0.39 mmol, 1.0 equ) and stirred for 30 min. DIPEA (0.13 mL, 0.78 mmol, 2.0 equ) was added and the resulting mixture stirred at room temperature overnight. The crude mixture was purified by preparative HPLC under acidic conditions, using 0.1% HCOOH in water:acetonitrile (5-95%) gradient elution to afford N-(4,4-difluorocyclohexyl)-2-((6-fluoro-4-oxo-3,4-dihydroquinazolin-2-yl)thio)acetamide as a white powder **26** (12 mg, 8.2% yield).  $C_{16}H_{16}N_3F_3O_2S$ , MW 371.86;  $^1H$  NMR (500 MHz, DMSO)  $\delta$  12.76 (brs, 1H), 8.39 - 8.36 (m, 1H), 7.71 - 7.60 (m, 2H), 7.52 (dd,  $J$  = 5.0, 8.9 Hz, 1H), 3.88 (s, 2H), 3.77 (d,  $J$  = 8.5 Hz, 1H), 2.08 - 1.77 (m, 6H), 1.55 - 1.47 (m, 2H). LCMS  $m/z$  372.3,  $[M + H]^+$  100%. HRMS ( $m/z$ ):  $[M + H]^+$  calcd for  $C_{16}H_{17}N_3F_3O_2S$ , 372.0988; found 372.0987.

**2-Thioxo-2,3-dihydropyrido[3,4-d]pyrimidin-4(1H)-one (36).** 2-Aminopyridine-4-carboxylic acid **35** (1 g, 7.2 mmol, 1.0 equ) and thiourea (2.8 g, 36.2 mmol, 5.0 equ) were heated neat in a round-bottom flask to 180°C for 3h with stirring. The reaction was cooled and 25 ml of water added. After stirring for 10 min the precipitate formed was filtered off, washed with cold water and dried to afford 2-thioxo-2,3-dihydropyrido[3,4-d]pyrimidin-4(1H)-one **36** (1.11 g, 85% yield) as a yellow powder.  $C_7H_5FN_2OS$ , MW 179.2;  $^1H$  NMR (500 MHz, DMSO)  $\delta$  12.89 (brs, 1H), 12.70 (brs, 1H), 8.73 (s, 1H), 8.49 (d,  $J$  = 4.85 Hz, 1H), 7.79 (d,  $J$  = 0.80 Hz, 1H). LCMS  $m/z$  180.11  $[M + H]^+$  100%.

**2-((4-Oxo-3,4-dihydropyrido[3,4-d]pyrimidin-2-yl)thio)acetic acid (37).** 2-thioxo-2,3-dihydropyrido[3,4-d]pyrimidin-4(1H)-one **36** (500 mg, 2.79 mmol, 1.0 equ), 2-bromoacetic acid (775.39 mg, 5.5 mmol, 2.0 equ) and triethylamine (2.33 mL, 16.7 mmol, 6.0 equ) were stirred in DMF (5 mL) at 75°C for 12 hr. Upon reaction completion the reaction mixture was poured over crushed ice, acidified with 1N HCl and the precipitate collected and dried to afford 2-((4-oxo-3,4-dihydropyrido[3,4-d]pyrimidin-2-yl)thio)acetic acid **37** (600 mg, 90.6% yield). C<sub>9</sub>H<sub>7</sub>N<sub>3</sub>O<sub>3</sub>S, MW 237.24; <sup>1</sup>H NMR (500 MHz, DMSO) δ 12.89 (s, 1H), 8.85 (d, *J* = 0.65 Hz, 1H), 8.57 (d, *J* = 5.00 Hz, 1H), 7.88 (d, *J* = 0.80 Hz, 1H), 4.08 (s, 2H). LCMS *m/z* 238.15 [M + H]<sup>+</sup> 100%.

**N-(4,4-Difluorocyclohexyl)-2-((4-oxo-3,4-dihydropyrido[3,4-d]pyrimidin-2-yl)thio)acetamide (27).** White powder (64 mg, 42% yield), C<sub>15</sub>H<sub>16</sub>N<sub>4</sub>O<sub>2</sub>F<sub>2</sub>S, MW 354.38; <sup>1</sup>H NMR (500 MHz, DMSO) δ 13.02 (s, 1H), 8.86 (s, 1H), 8.57 (d, *J*=5.2 Hz, 1H), 8.29 (d, *J*=7.4 Hz, 1H), 7.87 (d, *J*=5.0 Hz, 1H), 3.98 (s, 2H), 3.31 (s, 1H), 2.09 - 1.99 (m, 2H), 1.98 - 1.86 (m, 2H), 1.86 - 1.77 (m, 2H), 1.58 - 1.48 (m, 2H). LCMS *m/z* 355.22 [M + H]<sup>+</sup> 100%. HRMS (*m/z*): [M + H]<sup>+</sup> calcd for C<sub>15</sub>H<sub>17</sub>N<sub>4</sub>O<sub>2</sub>F<sub>2</sub>S, 355.1034; found 355.1033.

**Intrinsic clearance (Cli) experiments.** Test compound (0.5μM) was incubated with female CD1 mouse liver microsomes (Xenotech LLC <sup>TM</sup>; 0.5mg/mL 50mM potassium phosphate buffer, pH7.4) and the reaction started with addition of excess NADPH (8mg/mL 50mM potassium phosphate buffer, pH7.4). Immediately, at time zero, then at 3, 6, 9, 15 and 30 minutes an aliquot (50 μL) of the incubation mixture was removed and mixed with acetonitrile (100uL) to stop the reaction. Internal standard was added to all samples, the samples centrifuged to sediment precipitated protein and the plates then sealed prior to UPLCMSMS analysis using a Quattro Premier XE (Waters Corporation, USA). Xlfit (IDBS, UK) was used to calculate the exponential decay and consequently the rate constant (*k*) from the ratio of peak area of test compound to internal standard at each timepoint. The rate of intrinsic clearance (Cli) of each test compound was then calculated using the following calculation:

$$CLi(\text{mL/min/g liver}) = k \times V \times \text{microsomal protein yield}$$



Where V (mL/mg protein) is the incubation volume/mg protein added and microsomal protein yield is taken as 52.5mg protein/g liver. Verapamil (0.5  $\mu$ M) was used as a positive control to confirm acceptable assay performance.

**Aqueous solubility.** The aqueous solubility of the test compounds was measured using laser nephelometry. Compounds were subject to serial dilution from 10 mM to 0.5 mM in DMSO. An aliquot was then mixed with MilliQ water to obtain an aqueous dilution plate with a final concentration range of 250 – 12  $\mu$ M, with a final DMSO concentration of 2.5%. Triplicate aliquots were transferred to a flat bottomed polystyrene plate which was immediately read on the NEPHELOstar (BMG Lab Technologies). The amount of laser scatter caused by insoluble particulates (relative nephelometry units, RNU) was plotted against compound concentration using a segmental regression fit, with the point of inflection being quoted as the compounds aqueous solubility ( $\mu$ M).

**CHI Log D determination.** The chromatographic hydrophobicity index (CHI) was determined according the method previously described<sup>43-44</sup>. Briefly, test compounds were prepared as 0.5 mM solutions in 50:50 acetonitrile:water and analysed by reversed-phase HPLC-UV (wavelength 254 nm) using a Phenomenex Luna C18 100Å 150x4.6mm 5 micron column with a gradient of aqueous phase (50 mM ammonium acetate (pH 7.4)) and mobile phase (acetonitrile). By plotting the retention time of a set of reference compounds against known CHI values, the CHI value of test compounds were calculated according to their retention time.

**Plasma protein binding experiments.** In brief, a 96 well equilibrium dialysis apparatus was used to determine the free fraction in plasma for each compound (HT Dialysis LLC, Gales Ferry, CT). Membranes (12-14 kDA cut-off) were conditioned in deionised water for 60 minutes, followed by conditioning in 80:20 deionised water : ethanol overnight and then rinsed in water and isotonic buffer before use. Mouse plasma from appropriate species was removed from the freezer and allowed to thaw on the day of experiment. Thawed plasma was then centrifuged (Allegra X12-R, Beckman Coulter, USA), spiked with test

compound (final concentration 10 µg/mL), and 150 µL aliquots (n=3 replicate determinations) loaded into the 96-well equilibrium dialysis plate. Dialysis against isotonic buffer (150 µL) was carried out for 5 hours in a temperature controlled incubator at ca. 37°C (Barworld scientific Ltd, UK) using an orbital microplate shaker at 100 revolutions/minute (Barworld scientific Ltd, UK). At the end of the incubation period, 50 µL aliquots of plasma or buffer were transferred into a 96 well deep plate and the composition in each well balanced with control fluid (50 µL), such that the volume of buffer to plasma is the same. Sample extraction was performed by the addition of 200 µL of acetonitrile containing an appropriate internal standard. Samples were allowed to mix for 1 minute and then centrifuged at 3000 rpm in 96-well blocks for 15 minutes (Allegra X12-R, Beckman Coulter, USA) after which 150 µL of supernatant was removed to 50 µL of water.. All samples were analysed by UPLC-MS/MS on a Quattro Premier XE Mass Spectrometer (Waters Corporation, USA). The unbound fraction was determined as the ratio of the peak area in buffer to that in plasma.

**PAMPA assay.** The permeability was performed using a 96-well pre-coated BD Gentest™ PAMPA plate (BD Biosciences, U.K.). Each well was divided into two chambers; donor and acceptor, separated by a lipid-oil-lipid tri-layer constructed in a porous filter. The effective permeability,  $P_e$ , of the compound was measured at pH 7.4. Stock solutions (5 mM) of the compound were prepared in DMSO. The compound was then further diluted to 10 µM in phosphate buffered saline at pH 7.4. The final DMSO concentration did not exceed 5 % v/v. The compound dissolved in phosphate buffered saline was then added to the donor side of the membrane and phosphate buffered saline without compound was added to the acceptor side. The PAMPA plate was left at room temperature for 5 h, after which time, an aliquot (100 µl) was then removed from both acceptor and donor compartments and mixed with acetonitrile (80 µl) containing an internal standard: Donepezil at 50 ng/ml). The samples were centrifuged (10 min, 5°C, 3270 g) to sediment precipitated protein and sealed prior to UPLC-MS/MS analysis using a Quattro Premier XE (Waters Corp, USA).  $P_e$  was calculated as shown in the below equation:

$$Pe \text{ (nm/sec)} = \frac{107}{x} \times -\ln [1 - CA(t) / Ce_{eqi}]$$

$$A * (1/VD + 1/VA) * t$$

Where:

CA(t) = peak area of compound present in acceptor well at time t = 18000 sec

Ce<sub>qui</sub> = [CD(t) \* VD + CA(t) \* VA] / (VD + VA)

A = filter area

VD = donor well volume

VA = acceptor well volume

t = incubation time

CD(t) = peak area of compound present in donor well at time t = 18000 sec

Recovery of compound from donor and acceptor wells was calculated and data was only accepted when recovery exceeded 70 %.

**Animal care assurance:** All mouse studies performed at the University of Dundee were performed under the authority of a project license (PPL70/8346) issued by the Home Office under the Animals (Scientific Procedures) Act 1986, as amended in 2012 (and in compliance with EU Directive EU/2010/63). License applications are approved by the University's Ethical Review Committee (ERC) before submission to the Home Office. The ERC develops and oversees policy on all aspects of the use of animals on University premises and is a sub-committee of the University Court, its highest governing body.

**Mouse pharmacokinetics:** Test compound was dosed as a bolus solution intravenously at 3mg free base/kg (dose volume: 5 mL/kg; dose vehicle: 10% DMSO; 40% PEG400; 50% saline) to female C57Bl/6 mice (n=3) or dosed orally by gavage as a suspension at 10 or at 5, 30 or 100mg free base/kg (dose volume: 10mL/kg; dose vehicle: 1.0% carboxy methyl cellulose) to female C57Bl/6 mice (n=3/dose level). Blood samples were taken from each mouse tail vein at predetermined time points post-dose, mixed with nine volumes of distilled water and stored frozen until UPLC/MS/MS analysis. Pharmacokinetic parameters were derived from the blood concentration time curve using PK Solutions software v 2.0 (Summit Research Services, USA).

**Strains and media.** *Mycobacterium tuberculosis* H37Rv (ATCC 27294) was used for all work with this organism unless otherwise indicated. The activity of the compound on cell wall synthesis and the *bc<sub>1</sub>*

complex was measured using the *piniBAC* reporter strain and the *cydC::aph* strains, respectively, using previously described methods<sup>35, 45</sup>. Broth-based medium (7H9/ADC/Tw) for *MTb* consisted of Middlebrook 7H9 (Becton Dickinson) supplemented with ADC [albumin (50 g/ L)/dextrose (20 g/ L)/NaCl (8.1 g/ L)], 0.2% glycerol] and 0.05% Tween 80. Solid growth medium for *MTb* was Middlebrook 7H11 (Becton Dickinson) supplemented with OADC [ADC with 0.06% oleic acid]. Potencies of compounds by MIC determination were performed as previously described<sup>45</sup>. The  $\Delta ndhA$  strain was generated by insertion of the *aph* gene into the native *Bam*HI restriction site 873 nucleotides downstream of the start codon using previously described suicide vector method<sup>46</sup> to effect legitimate recombination in *MTb*.

**Measurement of intracellular ATP levels.** *MTb* H37Rv was grown to early-log phase (OD<sub>650nm</sub> of 0.2) and diluted 20-fold in the same medium (7H9/ADC/Tw). 100  $\mu$ L aliquots of cells were added to each well of sterile white polystyrene 96-well plates (Corning Inc., Corning, NY) containing 2  $\mu$ L drug dilutions in DMSO in triplicate. ATP was measured at different time points as indicated by a bioluminescent assay using the BacTiter-Glo reagent (Promega, Madison, WI) as recommended by the manufacturer.

**Bioenergetics.** The extracellular flux analysis assays were performed as described previously<sup>21, 36</sup>. In short, *M. tuberculosis* H37Rv were grown in 7H9 (10% OADC, 0.01% tyloxapol) to an OD of 0.8. Bacilli were pelleted, suspended in unbuffered carbon-source-free XF 7H9 media and seeded into the XF culture plate, at a density of  $2 \times 10^6$  bacilli/well. During the XF screen, the oxygen consumption rate (OCR) was measured, non-invasively and in real time. OCR data points are representative of the average OCR during 3 minutes of continuous measurement in the transient microchamber, with the error being calculated from the OCR measurements taken from eight replicate wells by the Wave Desktop 2.3 software (Agilent). During the assay carbon sources (glucose and palmitate at a final concentration of 0.2%), the mercapto-quinazolinones (Compounds **1** and **7** at final concentrations of 39 and 45  $\mu$ M respectively) and CCCP (final concentration of 3  $\mu$ M) was added to the assay media at the indicated time.

**Inverted membrane vesicles (IMV).** IMVs were isolated and the ATP generation assay performed as described previously<sup>36</sup>. In brief, *MTb* mc<sup>2</sup>6230 (cultured in 7H9, 0.01% tyloxapol, 10% OADC, 0.2% casamino acids and 24 µg/ml pantothenic acid) were collected via centrifugation, incubated with lysozyme and lysed via bead beating in a buffer containing 10mM HEPES, 50mM KCl, 5mM MgCl<sub>2</sub>, and 10% glycerol. IMV's were isolated by differential centrifugation. ATP synthesis assay was performed using a Roche Bioluminescence Assay Kit CL II. Membrane vesicles were provided either 250 µM NADH or 1mM succinate as an electron donor, 50 µM ADP, and 5 mM phosphate in the above buffer containing the luciferase/luciferin reagents. Luminescence was measured in a 384-well plate using a BioTek Synergy H4 plate reader.

**Recombinant Rv1854c purification.** The ORF corresponding to Rv1854c was codon optimized for *E. coli*, synthesized (ThermoFisher), and cloned between the NcoI and HindIII sites of pMALc5x, affording a vector for the IPTG-inducible over-expression of MtNdh with an N-terminal maltose-binding protein (MBP) fusion tag. This vector was transformed into *E. coli* BL21 (DE3) pLysS, and protein expression achieved in 1 L of media (ZYM + 0.1 % glucose, 0.1 % glycerol, 2 mM MgSO<sub>4</sub>, 34 µg/ml chloramphenicol, 50 µg/ml carbenicillin) following induction with 0.3 mM IPTG at 37°C for 4 h. Cells were harvested, resuspended in 40 ml buffer A (50 mM HEPES 100 mM KPO<sub>4</sub> pH 7.1, 5 % (w/v) glycerol) with added 5 U/mL DNase, complete protease inhibitor, 5 µM FAD, 10 mM MgCl<sub>2</sub>, and 0.25 % CHAPS, and sonicated on ice to lyse. Following centrifugation at 20,000 G for 30 min, the soluble fraction was incubated with 2 mL settled volume of pre-equilibrated (buffer A + 0.25 % CHAPS) amylose resin for 30 minutes at 4°C, and then applied to a gravity flow column. The resin was washed with 15 CV buffer A + 0.25 % CHAPS, then 15 CV buffer A without CHAPS. Bound protein was eluted with 10 mL buffer A + 20 mM maltose. The same purification procedure was repeated twice on the initial resin flow-throughs, all eluates combined, and concentrated using spin columns. The concentrated prep was then passed through a Superdex 75 10/300 column (running buffer was buffer A), and relevant fractions collected and concentrated. Aliquots of the resulting weakly-yellow solution were flash frozen and stored at -80°C until needed. Protein concentration was measured by spectrophotometric flavin (FAD) analysis, as described by<sup>47</sup>.

**Ndh activity assays.** MtNdh catalytic activity was measured by monitoring NADH oxidation at 340 nm ( $\epsilon = 6,220 \text{ M}^{-1} \text{ cm}^{-1}$ ) in a UV-Vis spectrophotometer at RT. Reactions (1 mL) consisted of 0.1 M HEPES pH 7.0, 10 % DMSO, 0.1-0.5 nM recombinant MBP-MtNdh and varying concentrations of Q2 and NADH. Reactions were started by addition of NADH, following ~1 min preincubation of all other reaction components. Kinetic data was taken at steady-state within the first 1 minute of the reaction. Background NADH oxidation in the absence of Q2 was measured (typically <5 % of rate with Q2 present) and subtracted from all subsequent measurements, as required. All kinetic data was plotted and analysed using GraphPad Prism software.

**SUPPLEMENTARY FILES**

Supplementary files describe the following:

1. Compound syntheses and characterization,
2. Met-ID studies of compounds **1** and **7** with microsomes with and without GSH,
3. graphs showing metabolic transformations in Met-ID studies,
4. pharmacokinetic studies, anaerobic cidal and intra-macrophage activity of compound **1**, and
5. whole genome sequencing methods and data table.

**ACKNOWLEDGEMENTS**

This work was funded in part by the Intramural Research Program of NIAID (AI000693-25), by grants from the Foundation for the National Institutes of Health (BARRY11HTB0) with support from the Bill & Melinda Gates Foundation (OPP1024021), and by the South African Medical Research Council (SAMRC) with funds received from Strategic Health Innovation Partnerships (SHIP) unit of the SAMRC; by the National Research Foundation of South Africa; and OPP1066891 - "A Centre of Excellence for Lead Optimization for Diseases of the Developing World" a joint award from the Wellcome Trust and the Bill & Melinda Gates Foundation. AJCS is a Burroughs Wellcome Investigator in the Pathogenesis of Infectious Diseases. PMF was a Howard Hughes Medical Institute Medical Research Fellow. We thank David Gray, James Roberts and Alastair Pate for support with data analysis, compound handling and data management.

## ABBREVIATIONS

NDH-2, type II NADH dehydrogenase; *MTb*; *Mycobacterium tuberculosis*; MtNdh, *MTb* NDH-2; SAR, structure-activity relationships; Kan, kanamycin; INH, isoniazid; RIF, rifampicin; MDR-TB, multi-drug resistant TB; XDR-TB, extensively drug-resistant tuberculosis; MoA, mechanism of action; MIC, minimum inhibitory concentration; AUC, area under the curve; IMVs, inverted membrane vesicles; OCR, oxygen consumption rate; LLE, ligand-lipophilicity efficiency; ADME, absorption, distribution, metabolism, and excretion; met-ID, metabolite identification; cLogP, calculated logP; Cli, intrinsic clearance; RLU, Relative fluorescence units; CFU, colony-forming units; OXPHOS, oxidative phosphorylation; CCCP, carbonyl cyanide m-chlorophenyl hydrazine; ETC, electron transport chain; CPZ, chlorpromazine.

## AUTHOR INFORMATION

HIMB, DFW, KA, and KYR performed biological experiments on *MTb*; TRI, JS performed sequencing analysis of resistant mutants; GAP performed enzyme assays; DAL, PMF and AJCS performed and analyzed bioenergetics; DM, PCR, TB, JRH, KG, CSM, TSF, LJS, KC synthesized compounds; PS, LE, JR, YS, LF, MOC, OE and KDR performed ADME/PK analysis; HIMB, SRG, CEB, PCR, PW and VM helped with data interpretation; PCR, HIMB and SRG wrote the manuscript, DW, TSF, CSM, CEB and DM edited the manuscript which was reviewed by all authors.

## CONFLICT OF INTEREST

The authors declare no conflict of interest.

## REFERENCES

1. WHO *Global tuberculosis report 2015*; ISBN 978-92-4-156505-9; World Health Organization: Geneva (Switzerland), 2015.
2. WHO *Treatment of tuberculosis: guidelines*; ISBN 978-92-4-154783-3; World Health Organization: Geneva (Switzerland), 2010.

3. Horsburgh, C. R. J.; Barry, C. E. I.; Lange, C., Treatment of Tuberculosis. *New England Journal of Medicine* **2015**, 373 (22), 2149-2160. DOI: doi:10.1056/NEJMra1413919.

4. Iseman , M. D., Treatment of Multidrug-Resistant Tuberculosis. *New England Journal of Medicine* **1993**, 329 (11), 784-791. DOI: 10.1056/nejm199309093291108.

5. Migliori, G. B.; Loddenkemper, R.; Blasi, F.; Raviglione, M. C., 125 years after Robert Koch's discovery of the tubercle bacillus: the new XDR-TB threat. Is “science” enough to tackle the epidemic? *European Respiratory Journal* **2007**, 29 (3), 423-427. DOI: 10.1183/09031936.00001307.

6. Velayati, A. A.; Masjedi, M. R.; Farnia, P.; Tabarsi, P.; Ghanavi, J.; ZiaZarifi, A. H.; Hoffner, S. E., Emergence of New Forms of Totally Drug-Resistant Tuberculosis Bacilli: Super Extensively Drug-Resistant Tuberculosis or Totally Drug-Resistant Strains in Iran. *Chest* **2009**, 136 (2), 420-425. DOI: 10.1378/chest.08-2427.

7. Schluger, N. W., Drug-Resistant Tuberculosis. *Chest* **2009**, 136 (2), 333-335. DOI: 10.1378/chest.09-0785.

8. Palomino, J. C.; Martin, A., Drug Resistance Mechanisms in Mycobacterium tuberculosis. *Antibiotics* **2014**, 3 (3), 317-340. DOI: 10.3390/antibiotics3030317.

9. Zumla, A. I.; Gillespie, S. H.; Hoelscher, M.; Philips, P. P. J.; Cole, S. T.; Abubakar, I.; McHugh, T. D.; Schito, M.; Maeurer, M.; Nunn, A. J., New antituberculosis drugs, regimens, and adjunct therapies: needs, advances, and future prospects. *The Lancet Infectious Diseases* **2014**, 14 (4), 327-340. DOI: 10.1016/S1473-3099(13)70328-1.

10. Selassie, A. W.; Pozsik, C.; Wilson, D.; Ferguson, P. L., Why Pulmonary Tuberculosis Recurs: A Population-based Epidemiological Study. *Annals of Epidemiology* **2005**, 15 (7), 519-525. DOI: 10.1016/j.annepidem.2005.03.002.

11. Owens, J. P.; Fofana, M. O.; Dowdy, D. W., Cost-effectiveness of novel first-line treatment regimens for tuberculosis. *The International Journal of Tuberculosis and Lung Disease* **2013**, 17 (5), 590-596. DOI: 10.5588/ijtld.12.0776.



12. Lienhardt, C.; Vernon, A.; Raviglione, M. C., New drugs and new regimens for the treatment of tuberculosis: review of the drug development pipeline and implications for national programmes. *Current Opinion in Pulmonary Medicine* **2010**, *16* (3), 186-193. DOI: 10.1097/MCP.0b013e328337580c.
13. Cole, S. T., Inhibiting *Mycobacterium tuberculosis* within and without. *Philosophical Transactions of the Royal Society B: Biological Sciences* **2016**, *371* (1707). DOI: 10.1098/rstb.2015.0506.
14. Ioerger, T. R.; O'Malley, T.; Liao, R.; Guinn, K. M.; Hickey, M. J.; Mohaideen, N.; Murphy, K. C.; Boshoff, H. I. M.; Mizrahi, V.; Rubin, E. J.; Sasseti, C. M.; Barry, C. E.; Sherman, D. R.; Parish, T.; Sacchettini, J. C., Identification of New Drug Targets and Resistance Mechanisms in *Mycobacterium tuberculosis*. *PLoS ONE* **2013**, *8* (9), e75245. DOI: 10.1371/journal.pone.0075245.
15. Zhang, Yanjia J.; Reddy, Manchi C.; Ioerger, Thomas R.; Rothchild, Alissa C.; Dartois, V.; Schuster, Brian M.; Trauner, A.; Wallis, D.; Galaviz, S.; Huttenhower, C.; Sacchettini, James C.; Behar, Samuel M.; Rubin, Eric J., Tryptophan Biosynthesis Protects Mycobacteria from CD4 T-Cell-Mediated Killing. *Cell* **2013**, *155* (6), 1296-1308. DOI: 10.1016/j.cell.2013.10.045.
16. Rao, S. P. S.; Alonso, S.; Rand, L.; Dick, T.; Pethe, K., The protonmotive force is required for maintaining ATP homeostasis and viability of hypoxic, nonreplicating *Mycobacterium tuberculosis*. *Proceedings of the National Academy of Sciences* **2008**, *105* (33), 11945-11950. DOI: 10.1073/pnas.0711697105.
17. DeJesus, M. A.; Gerrick, E. R.; Xu, W.; Park, S. W.; Long, J. E.; Boutte, C. C.; Rubin, E. J.; Schnappinger, D.; Ehrt, S.; Fortune, S. M.; Sasseti, C. M.; Ioerger, T. R., Comprehensive Essentiality Analysis of the *Mycobacterium tuberculosis* Genome via Saturating Transposon Mutagenesis. *mBio* **2017**, *8* (1). DOI: 10.1128/mBio.02133-16.
18. Heikal, A.; Hards, K.; Cheung, C.-Y.; Menorca, A.; Timmer, M. S. M.; Stocker, B. L.; Cook, G. M., Activation of type II NADH dehydrogenase by quinolinequinones mediates

antitubercular cell death. *Journal of Antimicrobial Chemotherapy* **2016**, *71* (10), 2840-2847. DOI: 10.1093/jac/dkw244.

19. Hong, W. D.; Gibbons, P. D.; Leung, S. C.; Amewu, R.; Stocks, P. A.; Stachulski, A.; Horta, P.; Cristiano, M. L. S.; Shone, A. E.; Moss, D.; Ardrey, A.; Sharma, R.; Warman, A. J.; Bedingfield, P. T. P.; Fisher, N. E.; Aljayyousi, G.; Mead, S.; Caws, M.; Berry, N. G.; Ward, S. A.; Biagini, G. A.; O'Neill, P. M.; Nixon, G. L., Rational Design, Synthesis, and Biological Evaluation of Heterocyclic Quinolones Targeting the Respiratory Chain of *Mycobacterium tuberculosis*. *Journal of Medicinal Chemistry* **2017**, *60* (9), 3703-3726. DOI: 10.1021/acs.jmedchem.6b01718.

20. Yano, T.; Kassovska-Bratinova, S.; Teh, J. S.; Winkler, J.; Sullivan, K.; Isaacs, A.; Schechter, N. M.; Rubin, H., Reduction of Clofazimine by *Mycobacterium* Type 2 NADH:Quinone Oxidoreductase: A PATHWAY FOR THE GENERATION OF BACTERICIDAL LEVELS OF REACTIVE OXYGEN SPECIES. *Journal of Biological Chemistry* **2011**, *286* (12), 10276-10287. DOI: 10.1074/jbc.M110.200501.

21. Moosa, A.; Lamprecht, D. A.; Arora, K.; Barry, C. E.; Boshoff, H. I. M.; Ioerger, T. R.; Steyn, A. J. C.; Mizrahi, V.; Warner, D. F., Susceptibility of *Mycobacterium tuberculosis* Cytochrome bd Oxidase Mutants to Compounds Targeting the Terminal Respiratory Oxidase, Cytochrome c. *Antimicrobial Agents and Chemotherapy* **2017**, *61* (10). DOI: 10.1128/aac.01338-17.

22. Alland, D.; Steyn, A. J.; Weisbrod, T.; Aldrich, K.; Jacobs, W. R., Characterization of the *Mycobacterium tuberculosis* iniBAC Promoter, a Promoter That Responds to Cell Wall Biosynthesis Inhibition. *Journal of Bacteriology* **2000**, *182* (7), 1802-1811. DOI: 10.1128/jb.182.7.1802-1811.2000.

23. Naran, K.; Moosa, A.; Barry, C. E.; Boshoff, H. I. M.; Mizrahi, V.; Warner, D. F., Bioluminescent Reporters for Rapid Mechanism of Action Assessment in Tuberculosis Drug Discovery. *Antimicrobial Agents and Chemotherapy* **2016**, *60* (11), 6748-6757. DOI: 10.1128/aac.01178-16.

24. Weinstein, E. A.; Yano, T.; Li, L.-S.; Avarbock, D.; Avarbock, A.; Helm, D.; McColm, A. A.; Duncan, K.; Lonsdale, J. T.; Rubin, H., Inhibitors of type II NADH:menaquinone oxidoreductase represent a class of antitubercular drugs. *Proceedings of the National Academy of Sciences of the United States of America* **2005**, *102* (12), 4548-4553. DOI: 10.1073/pnas.0500469102.
25. Sassetti, C. M.; Boyd, D. H.; Rubin, E. J., Genes required for mycobacterial growth defined by high density mutagenesis. *Molecular Microbiology* **2003**, *48* (1), 77-84. DOI: 10.1046/j.1365-2958.2003.03425.x.
26. McAdam, R. A.; Quan, S.; Smith, D. A.; Bardarov, S.; Betts, J. C.; Cook, F. C.; Hooker, E. U.; Lewis, A. P.; Woollard, P.; Everett, M. J.; Lukey, P. T.; Bancroft, G. J.; Jacobs, J., William R.; Duncan, K., Characterization of a Mycobacterium tuberculosis H37Rv transposon library reveals insertions in 351 ORFs and mutants with altered virulence. *Microbiology* **2002**, *148* (10), 2975-2986. DOI: doi:10.1099/00221287-148-10-2975.
27. Griffin, J. E.; Gawronski, J. D.; DeJesus, M. A.; Ioerger, T. R.; Akerley, B. J.; Sassetti, C. M., High-Resolution Phenotypic Profiling Defines Genes Essential for Mycobacterial Growth and Cholesterol Catabolism. *PLOS Pathogens* **2011**, *7* (9), e1002251. DOI: 10.1371/journal.ppat.1002251.
28. Leeson, P. D.; Young, R. J., Molecular Property Design: Does Everyone Get It? *ACS Medicinal Chemistry Letters* **2015**, *6* (7), 722-725. DOI: 10.1021/acsmedchemlett.5b00157.
29. Keseru, G. M.; Makara, G. M., The influence of lead discovery strategies on the properties of drug candidates. *Nat Rev Drug Discov* **2009**, *8* (3), 203-212. DOI: 10.1038/nrd2796.
30. Brown, M. F.; Avery, M.; Brissette, W. H.; Chang, J. H.; Colizza, K.; Conklyn, M.; DiRico, A. P.; Gladue, R. P.; Kath, J. C.; Krueger, S. S.; Lira, P. D.; Lillie, B. M.; Lundquist, G. D.; Mairs, E. N.; McElroy, E. B.; McGlynn, M. A.; Paradis, T. J.; Poss, C. S.; Rossulek, M. I.; Shepard, R. M.; Sims, J.; Strelevitz, T. J.; Truesdell, S.; Tylaska, L. A.; Yoon, K.; Zheng, D., Novel CCR1

antagonists with improved metabolic stability. *Bioorganic & Medicinal Chemistry Letters* **2004**, *14* (9), 2175-2179. DOI: 10.1016/j.bmcl.2004.02.022.

31. Swallow, S., Fluorine in Medicinal Chemistry. *Progress in Medicinal Chemistry* **2015**, *54*, 65-133. DOI: 10.1016/bs.pmch.2014.11.001.

32. Kalgutkar, A. S.; Dalvie, D., Predicting Toxicities of Reactive Metabolite–Positive Drug Candidates. *Annual Review of Pharmacology and Toxicology* **2015**, *55* (1), 35-54. DOI: doi:10.1146/annurev-pharmtox-010814-124720.

33. Stepan, A. F.; Walker, D. P.; Bauman, J.; Price, D. A.; Baillie, T. A.; Kalgutkar, A. S.; Aleo, M. D., Structural Alert/Reactive Metabolite Concept as Applied in Medicinal Chemistry to Mitigate the Risk of Idiosyncratic Drug Toxicity: A Perspective Based on the Critical Examination of Trends in the Top 200 Drugs Marketed in the United States. *Chemical Research in Toxicology* **2011**, *24* (9), 1345-1410. DOI: 10.1021/tx200168d.

34. Hartkoorn, R. C.; Uplekar, S.; Cole, S. T., Cross-Resistance between Clofazimine and Bedaquiline through Upregulation of MmpL5 in Mycobacterium tuberculosis. *Antimicrobial Agents and Chemotherapy* **2014**, *58* (5), 2979-2981. DOI: 10.1128/aac.00037-14.

35. Arora, K.; Ochoa-Montaña, B.; Tsang, P. S.; Blundell, T. L.; Dawes, S. S.; Mizrahi, V.; Bayliss, T.; Mackenzie, C. J.; Cleghorn, L. A. T.; Ray, P. C.; Wyatt, P. G.; Uh, E.; Lee, J.; Barry, C. E.; Boshoff, H. I., Respiratory Flexibility in Response to Inhibition of Cytochrome c Oxidase in Mycobacterium tuberculosis. *Antimicrobial Agents and Chemotherapy* **2014**, *58* (11), 6962-6965. DOI: 10.1128/aac.03486-14.

36. Lamprecht, D. A.; Finin, P. M.; Rahman, M. A.; Cumming, B. M.; Russell, S. L.; Jonnala, S. R.; Adamson, J. H.; Steyn, A. J. C., Turning the respiratory flexibility of Mycobacterium tuberculosis against itself. *Nature Communications* **2016**, *7*, 12393. DOI: 10.1038/ncomms12393.

37. Yano, T.; Rahimian, M.; Aneja, K. K.; Schechter, N. M.; Rubin, H.; Scott, C. P., Mycobacterium tuberculosis Type II NADH-Menaquinone Oxidoreductase Catalyzes Electron

Transfer through a Two-Site Ping-Pong Mechanism and Has Two Quinone-Binding Sites. *Biochemistry* **2014**, 53 (7), 1179-1190. DOI: 10.1021/bi4013897.

38. Shirude, P. S.; Paul, B.; Roy Choudhury, N.; Kedari, C.; Bandodkar, B.; Ugarkar, B. G., Quinolinylnyl Pyrimidines: Potent Inhibitors of NDH-2 as a Novel Class of Anti-TB Agents. *ACS Medicinal Chemistry Letters* **2012**, 3 (9), 736-740. DOI: 10.1021/ml300134b.

39. Yano, T.; Li, L.-S.; Weinstein, E.; Teh, J.-S.; Rubin, H., Steady-state Kinetics and Inhibitory Action of Antitubercular Phenothiazines on Mycobacterium tuberculosis Type-II NADH-Menaquinone Oxidoreductase (NDH-2). *Journal of Biological Chemistry* **2006**, 281 (17), 11456-11463. DOI: 10.1074/jbc.M508844200.

40. Heikal, A.; Nakatani, Y.; Dunn, E.; Weimar, M. R.; Day, C. L.; Baker, E. N.; Lott, J. S.; Sazanov, L. A.; Cook, G. M., Structure of the bacterial type II NADH dehydrogenase: a monotopic membrane protein with an essential role in energy generation. *Molecular Microbiology* **2014**, 91 (5), 950-964. DOI: 10.1111/mmi.12507.

41. Harbut, M. B.; Liu, R.; Yang, B.; Yano, T.; Vilcheze, C.; Lockner, J.; Guo, H.; Franzblau, S. G.; Petrassi, M.; Jacobs, W. R.; Rubin, H.; Chatterjee, A. K.; Wang, F., Small molecules targeting Mycobacterium tuberculosis type II NADH dehydrogenase with antimycobacterial activity. *Angewandte Chemie International Edition* **2018**, n/a-n/a. DOI: 10.1002/anie.201800260.

42. Vilchèze, C.; Weinrick, B.; Leung, L. W.; Jacobs, W. R., Plasticity of *Mycobacterium tuberculosis* NADH dehydrogenases and their role in virulence. *Proceedings of the National Academy of Sciences* **2018**. DOI: 10.1073/pnas.1721545115.

43. Camurri, G.; Zaramella, A., High-throughput liquid chromatography/mass spectrometry method for the determination of the chromatographic hydrophobicity index. *Analytical chemistry* **2001**, 73 (15), 3716-3722.

44. Valko, K.; Nunhuck, S.; Bevan, C.; Abraham, M. H.; Reynolds, D. P., Fast Gradient HPLC Method to Determine Compounds Binding to Human Serum Albumin. Relationships with

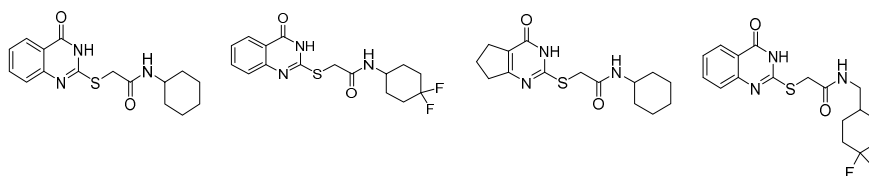
Octanol/Water and Immobilized Artificial Membrane Lipophilicity. *Journal of Pharmaceutical Sciences* **2003**, 92 (11), 2236-2248. DOI: 10.1002/jps.10494.

45. Park, Y.; Pacitto, A.; Bayliss, T.; Cleghorn, L. A. T.; Wang, Z.; Hartman, T.; Arora, K.; Ioerger, T. R.; Sacchettini, J.; Rizzi, M.; Donini, S.; Blundell, T. L.; Ascher, D. B.; Rhee, K.; Breda, A.; Zhou, N.; Dartois, V.; Jonnala, S. R.; Via, L. E.; Mizrahi, V.; Epemolu, O.; Stojanovski, L.; Simeons, F.; Osuna-Cabello, M.; Ellis, L.; MacKenzie, C. J.; Smith, A. R. C.; Davis, S. H.; Murugesan, D.; Buchanan, K. I.; Turner, P. A.; Huggett, M.; Zuccotto, F.; Rebollo-Lopez, M. J.; Lafuente-Monasterio, M. J.; Sanz, O.; Diaz, G. S.; Lelièvre, J.; Ballell, L.; Selenski, C.; Axtman, M.; Ghidelli-Disse, S.; Pflaumer, H.; Bösche, M.; Drewes, G.; Freiberg, G. M.; Kurnick, M. D.; Srikumaran, M.; Kempf, D. J.; Green, S. R.; Ray, P. C.; Read, K.; Wyatt, P.; Barry, C. E.; Boshoff, H. I., Essential but Not Vulnerable: Indazole Sulfonamides Targeting Inosine Monophosphate Dehydrogenase as Potential Leads against Mycobacterium tuberculosis. *ACS Infectious Diseases* **2017**, 3 (1), 18-33. DOI: 10.1021/acsinfecdis.6b00103.

46. Boshoff, H. I. M.; Reed, M. B.; Barry, C. E.; Mizrahi, V., DnaE2 Polymerase Contributes to In Vivo Survival and the Emergence of Drug Resistance in Mycobacterium tuberculosis. *Cell* **2003**, 113 (2), 183-193. DOI: 10.1016/S0092-8674(03)00270-8.

47. Aliverti, A.; Curti, B.; Vanoni, M. A., Identifying and Quantitating FAD and FMN in Simple and in Iron-Sulfur-Containing Flavoproteins. In *Flavoprotein Protocols*, Chapman, S. K.; Reid, G. A., Eds. Humana Press: Totowa, NJ, 1999; pp 9-23. DOI: 10.1385/1-59259-266-x:9.

## For Table of Contents Use Only



	<b>1</b>	<b>7</b>	<b>24</b>	<b>11</b>
<b>MIC (<math>\mu\text{M}</math>)</b>	0.3	0.4	1.5	0.8
<b>cLogP</b>	2.3	2.3	1.8	2.6
<b>Kin. Solubility (<math>\mu\text{M}</math>)</b>	83	105	>250	>250
<b>Microsomal Cli Mouse (mL/min/g)</b>	2.3	1.4	1.2	4.7